

Optimal Verification of the Bell State and Greenberger-Horne-Zeilinger States in Untrusted Quantum Networks

Yun-Guang Han,^{1,2,3} Zihao Li,^{1,2,3} Yukun Wang,⁴ and Huangjun Zhu^{1,2,3,*}

¹*State Key Laboratory of Surface Physics and Department of Physics, Fudan University, Shanghai 200433, China*

²*Institute for Nanoelectronic Devices and Quantum Computing, Fudan University, Shanghai 200433, China*

³*Center for Field Theory and Particle Physics, Fudan University, Shanghai 200433, China*

⁴*Department of Computer Science and Technology,
China University of Petroleum, Beijing 102249, China*

(Dated: December 28, 2021)

Bipartite and multipartite entangled states are basic ingredients for constructing quantum networks and their accurate verification is crucial to the functioning of the networks, especially for untrusted networks. Here we propose a simple approach for verifying the Bell state in an untrusted quantum network in which one party is not honest. Only local projective measurements are required for the honest party. It turns out each verification protocol is tied to a probability distribution on the Bloch sphere and its performance has an intuitive geometric meaning. This geometric picture enables us to construct the optimal and simplest verification protocols, which are also very useful to detecting entanglement in the untrusted network. Moreover, we show that our verification protocols can achieve almost the same sample efficiencies as protocols tailored to standard quantum state verification. Furthermore, we establish an intimate connection between the verification of Greenberger-Horne-Zeilinger states and the verification of the Bell state. By virtue of this connection we construct the optimal protocol for verifying Greenberger-Horne-Zeilinger states and for detecting genuine multipartite entanglement.

I. INTRODUCTION

Entanglement is the characteristic of quantum mechanics and key resource in quantum information processing [1–3]. As typical examples of bipartite and multipartite entangled states, the Bell state and Greenberger-Horne-Zeilinger (GHZ) states [4, 5] play crucial roles in numerous quantum information processing tasks and in foundational studies, such as quantum teleportation [6–8], quantum key distribution [9, 10], quantum random number generation [11], and nonlocality tests [12, 13]. Furthermore, as a special example of graph states [14], GHZ states are useful to constructing quantum networks [15, 16] designed for distributed quantum information processing, such as quantum secret sharing [17, 18], quantum conference key agreement [19] and distribution [20].

To guarantee the proper functioning of a quantum network, it is essential to verify the entangled state deployed in the network accurately and efficiently, especially for untrusted networks [21–29]. This scenario has wide applications in quantum information processing, such as one-sided device-independent (DI) quantum key distribution [30], anonymous communication [31, 32], and verifiable quantum secure modulo summation [33]. Meanwhile, this problem is tied to the foundational studies on quantum steering in the asymmetric scenario [3, 34–36] and the uncertainty principle in the presence of quantum memory [37, 38].

Unfortunately, not much is known about quantum verification in untrusted networks despite its significance.

This is because not all parties in the networks are honest, and the verification problem gets much more complicated in the presence of dishonest parties. In particular, traditional tomographic approaches are not applicable in the network setting even if their low efficiency is tolerable. Also, most alternative approaches, including direct fidelity estimation [39] and quantum state verification (QSV) [40–45], are not applicable, although QSV can address the adversarial scenario in which the source is not trustworthy [43–45]. DI QSV [46] based on self-testing [22, 47–52] can be applied in the network setting in principle, but is too resource consuming and too demanding with current technologies. For the Bell state and GHZ states, optimal verification protocols are known when all parties are honest [42, 53–58]. In the network setting, however, only suboptimal protocols are known in the literature [23–26, 29].

In this paper, we propose a simple approach for verifying the Bell state over an untrusted network in the semi-device-independent (SDI) scenario in which one party is not honest. Only local projective measurements are required for the honest party. In addition, we establish a simple connection between verification protocols of the Bell state and probability distributions on the Bloch sphere and reveal an intuitive geometric interpretation of the performance of each verification protocol. By virtue of this geometric picture, we construct the optimal and simplest protocols for verifying the Bell state, which can also be applied to detecting entanglement in the untrusted network. Moreover, we determine the sample efficiencies of our SDI verification protocols in addition to the guessing probabilities.

Furthermore, we establish an intimate connection between the verification of GHZ states and the verification

* zhu Huangjun@fudan.edu.cn

of the Bell state. Thanks to this connection, efficient protocols for verifying GHZ states can easily be constructed from the counterparts for the Bell state. Notably, this connection enables us to construct the optimal protocol for verifying GHZ states and for detecting genuine multipartite entanglement (GME). To put our work in perspective, we also provide a detailed comparison between SDI QSV considered in this work and standard QSV as well as DI QSV based on self-testing. For the Bell state and GHZ states, SDI verification can achieve almost the same sample efficiency as standard QSV; by contrast, the sample efficiency in the DI scenario is in general quadratically worse in the infidelity unless there exists a suitable Bell inequality for which the quantum bound coincides with the algebraic bound.

II. RESULTS

Verification of the Bell state

Suppose two distant parties, Alice and Bob, want to create the Bell state $|\Phi\rangle = (|00\rangle + |11\rangle)/\sqrt{2}$ as follows: Bob first prepares $|\Phi\rangle$ in his lab and then sends one particle of the entangled pair to Alice using a quantum channel. To verify this state Alice can perform a random projective measurement from a set of accessible measurements and then ask Bob to guess the measurement outcome given the measurement chosen. Each projective measurement is specified by a unit vector \mathbf{r} on the Bloch sphere, which specifies the two outcomes $P_{\pm} = (\mathbb{I} \pm \mathbf{r} \cdot \boldsymbol{\sigma})/2$, where $\boldsymbol{\sigma}$ is the vector composed of the three Pauli matrices. If Bob is honest and prepares the target state $|\Phi\rangle$, then his reduced states corresponding to the two outcomes P_+ and P_- have mutually orthogonal supports, so he can guess the measurement outcome with certainty by performing a suitable projective measurement.

If Bob is not honest and tries to prepare a different state ρ instead of $|\Phi\rangle$, then his *guessing probability*—the probability of successful guess—would be limited. In this case, Alice cannot distinguish two states that can be turned into each other by local operations of Bob; nevertheless, she can verify whether the state prepared is indeed $|\Phi\rangle$ up to these local operations. Let $\rho_{\pm} = \text{tr}_A(\rho P_{\pm})$ be the unnormalized reduced states of Bob. To guess the measurement outcome of Alice, Bob can perform a two-outcome POVM $\{E_+, E_-\}$ to distinguish ρ_+ and ρ_- . By the Helstrom theorem [59], the maximum guessing probability $\gamma(\rho, \mathbf{r})$ over all POVMs (or projective measurements) reads $\gamma(\rho, \mathbf{r}) = (1 + \|\rho_+ - \rho_-\|_1)/2$.

Recall that a general two-qubit state has the form

$$\rho = \frac{1}{4} \left(\mathbb{I} + \mathbf{a} \cdot \boldsymbol{\sigma} \otimes \mathbb{I} + \mathbb{I} \otimes \mathbf{b} \cdot \boldsymbol{\sigma} + \sum_{j,k} T_{jk} \sigma_j \otimes \sigma_k \right), \quad (1)$$

where σ_j, σ_k are Pauli matrices (also denoted by X, Y, Z), \mathbf{a} and \mathbf{b} are the Bloch vectors of the two reduced states, and T is the correlation matrix. If ρ is pure, then we can

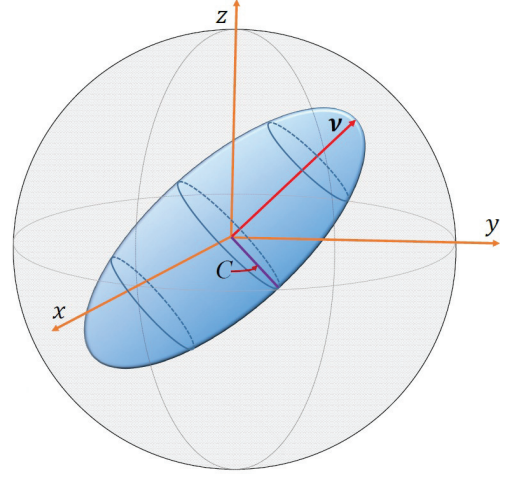


FIG. 1. Geometric illustration of the XYZ protocol in the Bloch sphere. For a given concurrence C , the guessing probability is maximized when the semi-major axis \mathbf{v} of the correlation ellipsoid parallels one of the eight intelligent directions.

deduce (cf. Supplementary Note 1),

$$\gamma(\rho, \mathbf{r}) = \frac{1}{2} (1 + \|T^T \mathbf{r}\|) = \frac{1}{2} (1 + \|\sqrt{TT^T} \mathbf{r}\|). \quad (2)$$

To understand the geometric meaning of $\gamma(\rho, \mathbf{r})$, note that the set of vectors $\{\sqrt{TT^T} \mathbf{r} : |\mathbf{r}| = 1\}$ forms a rotational ellipsoid, which is called the *correlation ellipsoid* and denoted by \mathcal{E}_ρ as illustrated in Fig. 1 (cf. the steering ellipsoid [60, 61]). The semi-major axis \mathbf{v} and semi-minor axis of \mathcal{E}_ρ have length 1 and C , respectively, where C is the concurrence of ρ [1, 62]. In addition, the radius $\|\sqrt{TT^T} \mathbf{r}\|$ is determined by C and the angle between \mathbf{r} and the semi-major axis as follows,

$$\|\sqrt{TT^T} \mathbf{r}\| = \|T^T \mathbf{r}\| = \sqrt{C^2 + (1 - C^2)(\mathbf{r} \cdot \mathbf{v})^2}. \quad (3)$$

A verification strategy of Alice is determined by a probability distribution μ on the Bloch sphere, which specifies the probability of performing each projective measurement. Given the strategy μ and the state ρ , the maximum average guessing probability of Bob reads

$$\gamma(\rho, \mu) := \int d\mu(\mathbf{r}) \gamma(\rho, \mathbf{r}) = \frac{1}{2} + \frac{1}{2} \int d\mu(\mathbf{r}) \|T^T \mathbf{r}\|, \quad (4)$$

where the bias is a weighted average of radii of the correlation ellipsoid. Denote by $\gamma_2(C, \mu)$ the maximum guessing probability over all pure states with concurrence at most C . Note that maximizing $\gamma(\rho, \mu)$ for a given concurrence amounts to choosing a proper orientation of the correlation ellipsoid so as to maximize the weighted average of radii, as illustrated in Fig. 1. This intuition leads to the following theorem as proved in Supplementary Note 1.

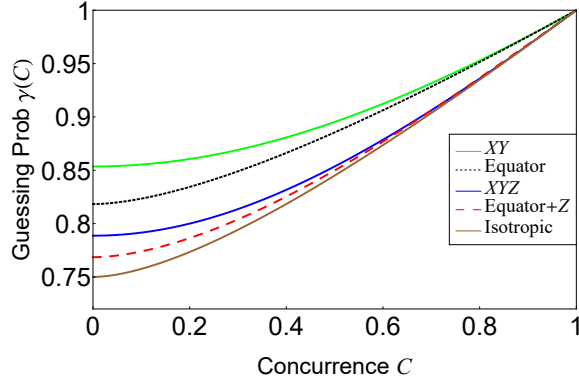


FIG. 2. The guessing probability $\gamma(C) = \gamma_2(C)$ as a function of the concurrence C for various verification protocols of the Bell state. Here the XY protocol and isotropic protocol are introduced in the main text, while other protocols are proposed in the Supplementary Material.

Theorem 1. Suppose $0 \leq C \leq 1$; then

$$\gamma_2(C, \mu) = \frac{1}{2}[1 + g(C, \mu)], \quad (5)$$

$$g(C, \mu) := \max_{\mathbf{v}} \int d\mu(\mathbf{r}) \sqrt{C^2 + (1 - C^2)(\mathbf{r} \cdot \mathbf{v})^2}, \quad (6)$$

where the maximization in Eq. (6) is over all unit vectors.

Any unit vector \mathbf{v} that maximizes the integration in Eq. (6) is called an *intelligent direction*. For a given concurrence, the guessing probability is maximized when the major axis of the correlation ellipsoid parallels an intelligent direction. When $C = 1$, the correlation ellipsoid is a sphere, in which case Theorem 1 yields $g(C, \mu) = 1$ and $\gamma_2(C, \mu) = 1$. When $C = 0$, the correlation ellipsoid reduces to a line segment, in which case we can deduce

$$g^*(\mu) := g(0, \mu) = \max_{\mathbf{v}} \int d\mu(\mathbf{r}) |\mathbf{r} \cdot \mathbf{v}|, \quad (7)$$

$$\gamma_2^*(\mu) := \gamma_2(0, \mu) = \frac{1}{2} + \frac{1}{2} \max_{\mathbf{v}} \int d\mu(\mathbf{r}) |\mathbf{r} \cdot \mathbf{v}|. \quad (8)$$

Notably, entanglement can be certified in the shared system when the guessing probability surpasses the threshold $\gamma_2^*(\mu)$. The relation between the guessing probability and concurrence for various verification protocols are illustrated in Fig. 2.

Alternative strategies of the adversary

So far we have assumed that the state ρ prepared by Bob is a two-qubit pure state and $\rho_A := \text{tr}_B(\rho)$ is supported in the local support of the target Bell state, that is, the subspace spanned by $|0\rangle$ and $|1\rangle$. Can Bob gain any advantage if ρ_A is not supported in this subspace? The answer turns out to be negative. Now Alice can first perform the projective measurement $\{P_A, \mathbb{I} - P_A\}$ with $P_A = |0\rangle\langle 0| + |1\rangle\langle 1|$ and then apply a verification protocol as before if she obtains the first outcome and reject

otherwise. The maximum guessing probability $\gamma(C, \mu)$ of Bob for any pure state with $C(\rho) \leq C$ is the same as before as shown in the following lemma and proved in Supplementary Note 3.

Lemma 1. $\gamma(C, \mu) = \gamma_2(C, \mu)$ for $0 \leq C \leq 1$.

Note that $\gamma(C, \mu) = 1$ when $C \geq 1$, in which case Bob can prepare the target Bell state. So we can focus on the case $0 \leq C \leq 1$. Define $\gamma^*(\mu) := \gamma(0, \mu)$, then $\gamma^*(\mu) = \gamma_2^*(\mu)$ thanks to Lemma 1, so the threshold for entanglement detection remains the same as before; cf. Eq. (8). In conjunction with the convexity of $\gamma_2(C, \mu)$ in C (cf. Lemma S1 in Supplementary Note 2), Lemma 1 implies that

$$\gamma(C, \mu) = \gamma_2(C, \mu) \leq \gamma^*(\mu)(1 - C) + C, \quad 0 \leq C \leq 1, \quad (9)$$

which offers the best linear upper bound for $\gamma(C, \mu)$. When the distribution μ is clear from the context, $\gamma_2^*(\mu)$ and $\gamma^*(\mu)$ are abbreviated as γ_2^* and γ^* for simplicity.

Above results can be extended to mixed states, although our main interest are pure states. Let $\hat{\gamma}(C, \mu)$ be the maximum guessing probability of Bob over all states with concurrence at most C . Define $\hat{\gamma}_2(C, \mu)$ in a similar way, but assuming that ρ_A is supported in the support of P_A . By the following theorem proved in Supplementary Note 4, $\hat{\gamma}(C, \mu)$ and $\hat{\gamma}_2(C, \mu)$ are weighted averages of $\gamma^*(\mu)$ and $\gamma(1, \mu) = 1$.

Theorem 2. Suppose $0 \leq C \leq 1$; then

$$\begin{aligned} \hat{\gamma}(C, \mu) &= \hat{\gamma}_2(C, \mu) = (1 - C)\gamma^*(\mu) + C \\ &= \frac{1 + C}{2} + \frac{1 - C}{2} \max_{\mathbf{v}} \int d\mu(\mathbf{r}) |\mathbf{r} \cdot \mathbf{v}|. \end{aligned} \quad (10)$$

Fidelity as the figure of merit

Next, we consider the fidelity as the figure of merit, which is more natural for QSV. Here we assume that Bob controls the whole system except that of Alice, so we can assume that the state ρ prepared by Bob is pure. Define the reduced fidelity

$$F_B(\rho) := \max_{U_B} \langle \Phi | (\mathbb{I}_A \otimes U_B) \rho (\mathbb{I}_A \otimes U_B)^\dagger | \Phi \rangle, \quad (11)$$

where the maximization is taken over all local unitary transformations on \mathcal{H}_B . Denote by $\gamma^F(F, \mu)$ the maximum guessing probability over all pure states with $F_B(\rho) \leq F$. Define $\gamma_2^F(F, \mu)$ in a similar way, but assuming that ρ_A is supported in the support of P_A . It is known that $F_B(\rho) = [1 + C(\rho)]/2 \geq 1/2$ for any two-qubit pure state ρ satisfying $P_A \rho_A = \rho_A$ [63]. So $\gamma_2^F(F, \mu)$ is defined only for $1/2 \leq F \leq 1$, although $\gamma^F(F, \mu)$ is defined for $0 \leq F \leq 1$.

The following theorem proved in Supplementary Note 5 clarifies the relations between $\gamma^F(F, \mu)$, $\gamma_2^F(F, \mu)$, and $\gamma_2(C, \mu)$. The guessing probabilities $\gamma^F(F, \mu)$ for various verification protocols are illustrated in Fig. 3.

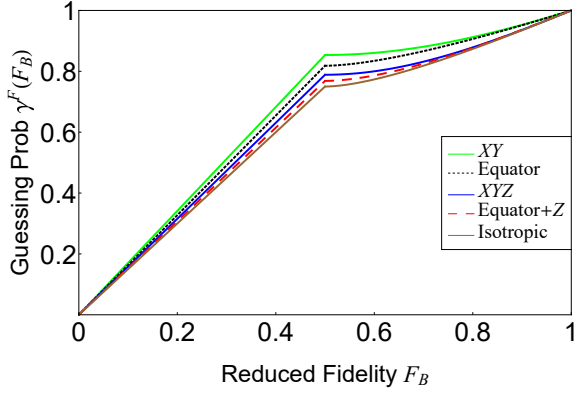


FIG. 3. Relation between the guessing probability $\gamma^F(F_B)$ and the reduced fidelity F_B for various verification protocols of the Bell state. Here the XY protocol and isotropic protocol are introduced in the main text, while other protocols are proposed in the Supplementary Material.

Theorem 3. Suppose $1/2 \leq F \leq 1$; then

$$\gamma_2^F(F, \mu) = \gamma_2(2F - 1, \mu) \leq 1 - 2(1 - \gamma^*)(1 - F). \quad (12)$$

Suppose $0 \leq F \leq 1$; then

$$\gamma^F(F, \mu) = \begin{cases} 2\gamma^*F & 0 \leq F < 1/2, \\ \gamma_2(2F - 1, \mu) & 1/2 \leq F \leq 1, \end{cases} \quad (13)$$

$$\gamma^F(F, \mu) \leq 1 - 2(1 - \gamma^*)(1 - F). \quad (14)$$

Equation (14) offers the best linear upper bound for $\gamma^F(F, \mu)$ when $1/2 \leq F \leq 1$ and demonstrates the robustness of the verification protocol. Theorems 1 to 3 corroborate the significance of the threshold γ^* in verifying the Bell state and entanglement in the SDI scenario. Moreover, the threshold γ^* determines the sample efficiency, as we shall see shortly. Therefore, γ^* can be regarded as the most important figure of merit for characterizing the performance of a verification protocol.

Simplest and optimal verification protocols

Here we propose several concrete verification protocols, including the simplest and optimal protocols. The main results are summarized in Table I and illustrated in Fig. 2; more technical details can be found in Supplementary Note 9.

In the simplest verification protocol, Alice can perform two projective measurements \mathbf{r}_1 and \mathbf{r}_2 with probabilities p_1 and p_2 , respectively. Here the maximum guessing probability $\gamma(C, \mu)$ only depends on the angle between \mathbf{r}_1 and \mathbf{r}_2 in addition to the probabilities p_1 and p_2 . Moreover, $\gamma(C, \mu)$ is minimized when $\mathbf{r}_1 \cdot \mathbf{r}_2 = 0$ and $p_1 = p_2 = 1/2$, in which case we have

$$g(C, \mu) = \sqrt{\frac{1+C^2}{2}}, \quad \gamma(C, \mu) = \frac{1}{2} + \frac{1}{2}\sqrt{\frac{1+C^2}{2}}, \quad (15)$$

and the guessing probability threshold is $\gamma^* = (2+\sqrt{2})/4$. When $\mathbf{r}_1 = (1, 0, 0)^T$ and $\mathbf{r}_2 = (0, 1, 0)^T$ for example,

we get the XY protocol. Previously, Ref. [23] proposed an equivalent protocol, but neither derived the exact formula for the guessing probability nor proved the optimality of the XY protocol among all two-setting protocols.

To determine the optimal protocol, we need to minimize $g(C, \mu)$ over μ . By Theorem 1 (cf. Lemma S1 in Supplementary Note 2), $g(C, \mu)$ is convex in μ , so $g(C, \mu)$ is minimized when μ is the uniform distribution on the Bloch sphere, which yields the *isotropic protocol* with

$$g(C, \mu) = \frac{1}{2} + \frac{C^2 \text{arcsinh}(\frac{\sqrt{1-C^2}}{C})}{2\sqrt{1-C^2}}, \quad (16)$$

$$\gamma(C, \mu) = \frac{3}{4} + \frac{C^2 \text{arcsinh}(\frac{\sqrt{1-C^2}}{C})}{4\sqrt{1-C^2}}, \quad (17)$$

and the guessing probability threshold is $\gamma^* = 3/4$.

Protocols based on the Pauli Z measurement and measurements on the xy -plane are of special interest to the verification of GHZ states as we shall see shortly. Prominent examples include the XYZ protocol (cf. Fig. 1), equator protocol, equator+Z protocol, polygon protocol, and polygon+Z protocol (see Supplementary Note 9).

Sample efficiency

To construct a practical verification protocol, it is crucial to clarify the sample efficiency. Although this problem has been resolved in standard QSV [42–44], little is known about the sample efficiency in the DI and SDI scenarios [46]. Here we clarify the sample efficiency of our verification protocols in the SDI scenario. Consider a quantum device that is supposed to produce the target state $|\Phi\rangle \in \mathcal{H}$, but actually produces the states $\rho_1, \rho_2, \dots, \rho_N$ in N runs. Our task is to verify whether these states are sufficiently close to the target state on average. Here the reduced fidelity is a natural choice for quantifying the closeness since Alice is ignorant to the local unitary transformations acting on Bob's system. To guarantee that the average reduced fidelity of the states $\rho_1, \rho_2, \dots, \rho_N$ is larger than $1 - \epsilon$ with significance level δ (confidence level $1 - \delta$), the number of tests required is determined in Supplementary Note 6, with the result

$$N = \left\lceil \frac{\ln \delta}{\ln[1 - 2(1 - \gamma^*)\epsilon]} \right\rceil \approx \frac{\ln \delta^{-1}}{2(1 - \gamma^*)\epsilon}. \quad (18)$$

Note that the sample efficiency is determined by the threshold $\gamma^* = \gamma_2^*$ defined in Eq. (8).

The minimum threshold $\gamma^* = 3/4$ is attained for the isotropic protocol, in which case $N \approx (2 \ln \delta^{-1})/\epsilon$, which is comparable to the number $(3 \ln \delta^{-1})/(2\epsilon)$ required in standard QSV [42, 53]. So the Bell state can be verified in the SDI scenario almost as efficiently as in the standard QSV. Our protocol can achieve the optimal sample complexity because it is tied to a steering inequality whose quantum bound coincides with the algebraic bound. In contrast, the sample complexity in the DI scenario is quadratically worse in the scaling with $1/\epsilon$, that is, $N \propto (\ln \delta^{-1})/\epsilon^2$ [46] (cf. Supplementary Note 7).

TABLE I. Concrete protocols for verifying the Bell state in an untrusted quantum network. Here $\gamma(C)$ ($\hat{\gamma}(C)$) is the maximum guessing probability for pure (mixed) states with concurrence at most C , and $\mathbf{v}(C=0)$ is an intelligent direction for $C=0$. Entanglement can be certified when the guessing probability surpasses the threshold $\gamma^* = \gamma(0) = \hat{\gamma}(0)$. The XY protocol and isotropic protocol are the simplest and optimal verification protocols, respectively. All protocols listed, except for the isotropic protocol, can be generalized to GHZ states.

Protocol	Threshold γ^*	$\gamma(C)$ (pure state)	$\hat{\gamma}(C)$ (mixed state)	$\mathbf{v}(C=0)$
XY	$\frac{1}{2} + \frac{1}{2\sqrt{2}} \approx 0.854$	$\frac{1}{2} + \frac{1}{2}\sqrt{\frac{1+C^2}{2}}$	$\frac{1}{4}[2 + \sqrt{2} + (2 - \sqrt{2})C]$	$\frac{1}{\sqrt{2}}(1, 1, 0)^T$
XYZ	$\frac{1}{2} + \frac{1}{2\sqrt{3}} \approx 0.789$	$\frac{1}{2} + \frac{1}{2}\sqrt{\frac{1+2C^2}{3}}$	$\frac{1}{6}[3 + \sqrt{3} + (3 - \sqrt{3})C]$	$\frac{1}{\sqrt{3}}(1, 1, 1)^T$
Isotropic	$\frac{3}{4} = 0.75$	$\frac{3}{4} + \frac{C^2 \operatorname{arcsinh}(\frac{\sqrt{1-C^2}}{C})}{4\sqrt{1-C^2}}$	$\frac{3+C}{4}$	any direction
Equator	$\frac{1}{2} + \frac{1}{\pi} \approx 0.818$	$\frac{1}{2} + \frac{1}{\pi}K(\sqrt{1-C^2})$	$\frac{1}{2\pi}[\pi + 2 + (\pi - 2)C]$	any direction in the xy -plane
Polygon(3)	$\frac{5}{6} \approx 0.833$	$\frac{4 + \sqrt{1+3C^2}}{6}$	$\frac{5+C}{6}$	any vertex direction
Equator + Z	$\frac{1}{2} + \frac{1}{\sqrt{4+\pi^2}} \approx 0.769$	—	$\frac{1+C}{2} + \frac{1-C}{\sqrt{4+\pi^2}}$	$\frac{1}{\sqrt{4+\pi^2}}(\pi, 0, 2)^T$
Polygon(3) + Z	$\frac{1}{2} + \frac{1}{\sqrt{13}} \approx 0.777$	—	$\frac{1}{2} + \frac{1}{\sqrt{13}} + (\frac{1}{2} - \frac{1}{\sqrt{13}})C$	$\frac{1}{\sqrt{13}}(3, 0, 2)^T$

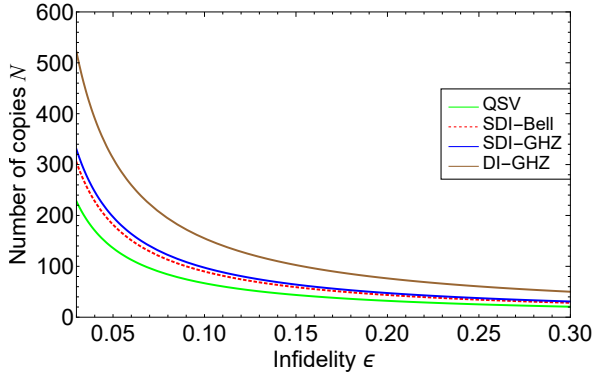


FIG. 4. Sample complexities for verifying the Bell state and GHZ states in three different scenarios. In standard QSV, the Bell state and GHZ states can be verified with the same sample complexity [42, 57]. In the SDI scenario, the isotropic protocol is chosen for verifying the Bell state and the optimized equator+Z protocol is chosen for verifying the GHZ states. In the DI scenario, the Mermin inequality is employed for verifying the three-qubit GHZ state [46, 50]. Here the significance level is chosen to be $\delta = 0.01$.

Verification of the GHZ state

Next, consider the GHZ state $|G^n\rangle = (|0\rangle^{\otimes n} + |1\rangle^{\otimes n})/\sqrt{2}$ of n -qubits with $n \geq 3$. To verify this state, the n parties can randomly perform certain tests based on local projective measurements. In each test, the verifier (one of the parties) asks each party to perform a local projective measurement as specified by a unit vector on the Bloch sphere and return the measurement outcome. If all parties are honest, then only the target state $|G^n\rangle$ can pass all tests with certainty, so the GHZ state can be verified. In the presence of dishonest parties, let \mathcal{D} be the set of dishonest parties, who know which parties are honest or dishonest and who may collude with each other; let \mathcal{H}

be the set of honest parties (including the verifier), who do not know which other parties are honest or dishonest. The goal is to verify $|G^n\rangle$ up to local unitary transformations on the joint Hilbert space of \mathcal{D} [23, 24]. Assuming $|\mathcal{D}|, |\mathcal{H}| \geq 1$, then $|G^n\rangle$ may be regarded as a Bell state shared between \mathcal{H} and \mathcal{D} . So the verification of the GHZ state is closely tied to the verification of the Bell state. Actually, there is no essential difference when $|\mathcal{H}| = 1$.

However, a key distinction arises when $|\mathcal{H}| \geq 2$ because each member of \mathcal{H} can only perform local projective measurements on his/her party. So the potential tests that the verifier can realize are restricted. Careful analysis in Supplementary Note 10 shows that only two types of tests for verifying the GHZ state $|G^n\rangle$ can be constructed from local projective measurements. In the first type, all parties perform Z measurements, and the test is passed if they obtain the same outcome. In this way the verifier can effectively realize the Z measurement on $V_{\mathcal{H}}$, where $V_{\mathcal{H}}$ is the two-dimensional subspace spanned by $\bigotimes_{j \in \mathcal{H}} |0\rangle_j$ and $\bigotimes_{j \in \mathcal{H}} |1\rangle_j$.

In the second type of tests, party j performs the $X(\phi_j)$ measurement with $\sum_j \phi_j = 0 \pmod{2\pi}$, where $X(\phi_j) = e^{-i\phi_j}|0\rangle\langle 1| + e^{i\phi_j}|1\rangle\langle 0|$ corresponds to the Bloch vector $(\cos \phi_j, \sin \phi_j, 0)^T$, and each ϕ_j is decided by the verifier. The test is passed if the number of outcomes -1 is even. Suppose $\phi_1, \phi_2, \dots, \phi_n$ are chosen independently and uniformly at random from the interval $[0, 2\pi)$. Then $\phi_{\mathcal{H}} := \sum_{j \in \mathcal{H}} \phi_j \pmod{2\pi}$ is uniformly distributed in $[0, 2\pi)$. Given $\phi \in [0, 2\pi)$, the average of $\bigotimes_{j \in \mathcal{H}} X(\phi_j)$ under the condition $\phi_{\mathcal{H}} = \phi$ reads

$$\left\langle \bigotimes_{j \in \mathcal{H}} X(\phi_j) \right\rangle_{\phi} = e^{-i\phi} \bigotimes_{j \in \mathcal{H}} (|0\rangle\langle 1|)_j + e^{i\phi} \bigotimes_{j \in \mathcal{H}} (|1\rangle\langle 0|)_j. \quad (19)$$

In this way, the verifier can effectively realize the $X(\phi)$ measurement on $V_{\mathcal{H}}$, where ϕ is completely random.

A similar result holds when ϕ_j are chosen independently and uniformly at random from the discrete set $\{2k\pi/M\}_{k=0}^{M-1}$ with $M \geq 3$ being a positive integer.

By the above analysis, the verifier can effectively realize projective measurements along the z -axis or on the xy -plane when represented on the Bloch-sphere of $V_{\mathcal{H}}$, but not other projective measurements (assuming $|\mathcal{H}| \geq 2$). Each verification protocol of the GHZ state corresponds to a probability distribution μ on the Bloch sphere that is supported on the equator together with the north and south poles. Moreover, for all protocols in Table I except for the isotropic protocol (cf. Supplementary Notes 9 and 10), the guessing probabilities are the same as in the verification of the Bell state. To be specific, $\gamma(C, \mu)$ and $\gamma^F(F, \mu)$ can be defined as before; Theorems 1, 3, and Lemma 1 still hold, except that now C refers to the bipartite concurrence between \mathcal{H} and \mathcal{D} . Although variants of the XY protocol and equator protocol were proposed previously [23, 24], such exact formulas for the guessing probabilities are not known in the literature. To optimize the performance, μ should be uniform on the equator, which leads to the equator+ Z protocol; the optimal probability p_Z for performing the Z measurement depends on C or F as before.

A quantum state ρ is genuinely multipartite entangled (GME) if its fidelity with the GHZ state $\text{tr}(\rho|G^n\rangle\langle G^n|)$ is larger than $1/2$ [64]. The GME can be certified if the guessing probability surpasses the detection threshold $\gamma^F(1/2) = \gamma^*$. This threshold is minimized at the special equator+ Z protocol with $p_Z = 4/(4 + \pi^2) \approx 0.288$, in which case we have

$$\gamma^F(1/2) = \gamma^* = \frac{1}{2} + \frac{1}{\sqrt{4 + \pi^2}} \approx 0.769. \quad (20)$$

This threshold is only 2.5% higher than the optimal threshold $3/4$ for certifying the entanglement of the Bell state based on the isotropic protocol.

The sample efficiency for verifying the GHZ state can be determined following a similar analysis applied to the Bell state. The formula in Eq. (18) still applies, except that the choice of verification protocols is restricted. Now the minimum of γ^* is achieved at a special equator+ Z protocol [cf. Eq. (20)]. So the GHZ state can be verified in the SDI scenario with almost the same efficiency as in the standard QSV [57], as illustrated in Fig. 4. In the DI scenario, by contrast, it is in general impossible to achieve such a high efficiency unless one can construct a Bell inequality for which the quantum bound coincides with the algebraic bound [46]. Notably, the three-qubit GHZ state can be verified with such a high efficiency by virtue of the Mermin inequality [46, 50].

It should be pointed out that all our protocols for verifying GHZ states are applicable even in the presence of an arbitrary number of dishonest parties as long as the verifier is honest. Meanwhile, these protocols are useful for detecting GME. For some cryptographic tasks such as anonymous quantum communication, the security for all honest parties can be guaranteed at the same time with the assistance of a trusted common random source (CRS) [23]. In this case, the number of honest parties can affect the security parameter.

III. DISCUSSION

We proposed a simple and practical approach for verifying the Bell state in an untrusted quantum network in which one party is not honest. We also established a simple connection between verification protocols of the Bell state and probability distributions on the Bloch sphere together with an intuitive geometric picture. Based on this connection, we derived simple formulas for the guessing probability as functions of the concurrence and reduced fidelity. Meanwhile, we clarified the sample efficiency of each verification protocol and showed that the sample efficiency is determined by the threshold in the guessing probability. Moreover, we constructed the optimal and simplest protocols for verifying the Bell state, which are also very useful to detecting entanglement in the untrusted network.

Furthermore, we reduce the verification problem of GHZ states to the counterpart of the Bell state, which enables us to construct the optimal protocol for verifying GHZ states and for detecting GME. Our work shows that both Bell state and GHZ states can be verified in the SDI scenario with the same sample complexity as in standard QSV. By contrast, the sample complexity in the DI scenario is in general quadratically worse. This work is instrumental to verifying entangled states in untrusted quantum networks, which is crucial to guaranteeing the proper functioning of quantum networks. In addition, this work is of intrinsic interest to the foundational studies on quantum steering. In the future, it would be desirable to generalize our results to generic bipartite pure states, stabilizer states, and other quantum states.

ACKNOWLEDGEMENTS

This work is supported by the National Natural Science Foundation of China (Grants No. 11875110 and No. 62101600) and Shanghai Municipal Science and Technology Major Project (Grant No. 2019SHZDZX01).

[1] Horodecki, R., Horodecki, P., Horodecki, M. & Horodecki, K. Quantum entanglement. *Rev. Mod. Phys.* **81**, 865–942 (2009).

[2] Brunner, N., Cavalcanti, D., Pironio, S., Scarani, V. & Wehner, S. Bell nonlocality. *Rev. Mod. Phys.* **86**, 419–478 (2014).

- [3] Uola, R., Costa, A. C. S., Nguyen, H. C. & Gühne, O. Quantum steering. *Rev. Mod. Phys.* **92**, 015001 (2020).
- [4] Greenberger, D. M., Horne, M. A. & Zeilinger, A. Going Beyond Bell's Theorem. in *Bell's Theorem, Quantum Theory and Conceptions of the Universe*, edited by Kafatos, M., 69–72, (Kluwer Academic, Dordrecht, 1989).
- [5] Greenberger, D. M., Horne, M. A., Shimony, A. & Zeilinger, A. Bell's theorem without inequalities. *Am. J. Phys.* **58**, 1131–1143 (1990).
- [6] Bennett, C. H. et al. Teleporting an unknown quantum state via dual classical and Einstein-Podolsky-Rosen channels. *Phys. Rev. Lett.* **70**, 1895–1899 (1993).
- [7] Bouwmeester, D. et al. Experimental quantum teleportation. *Nature* **390**, 575–579 (1997).
- [8] Zhao, Z. et al. Experimental demonstration of five-photon entanglement and open-destination teleportation. *Nature* **430**, 54–58 (2004).
- [9] Ekert, A. K. Quantum cryptography based on Bell's theorem. *Phys. Rev. Lett.* **67**, 661–663 (1991).
- [10] Acín, A. et al. Device-independent security of quantum cryptography against collective attacks. *Phys. Rev. Lett.* **98**, 230501 (2007).
- [11] Acín, A. & Masanes, L. Certified randomness in quantum physics. *Nature* **540**, 213–219 (2016).
- [12] Clauser, J. F., Horne, M. A., Shimony, A. & Holt, R. A. Proposed Experiment to Test Local Hidden-Variable Theories. *Phys. Rev. Lett.* **23**, 880–884 (1969).
- [13] Pan, J.-W., Bouwmeester, D., Daniell, M., Weinfurter, H. & Zeilinger, A. Experimental test of quantum nonlocality in three-photon Greenberger–Horne–Zeilinger entanglement. *Nature* **403**, 515–519 (2000).
- [14] Hein, M., Eisert, J. & Briegel, H. J. Multiparty entanglement in graph states. *Phys. Rev. A* **69**, 062311 (2004).
- [15] Kimble, H. J. The quantum internet. *Nature* **453**, 1023–1030 (2008).
- [16] Wehner, S., Elkouss, D. & Hanson, R. Quantum internet: A vision for the road ahead. *Science* **362**, eaam9288 (2018).
- [17] Hillery, M., Bužek, V. & Berthiaume, A. Quantum secret sharing. *Phys. Rev. A* **59**, 1829 (1999).
- [18] Bell, B. A. et al. Experimental demonstration of graph-state quantum secret sharing. *Nat. Commun.* **5**, 5480 (2014).
- [19] Zhao, S. et al. Phase-Matching Quantum Cryptographic Conferencing. *Phys. Rev. Appl.* **14**, 024010 (2020).
- [20] Fu, Y., Yin, H.-L., Chen, T.-Y. & Chen, Z.-B. Long-Distance Measurement-Device-Independent Multiparty Quantum Communication. *Phys. Rev. Lett.* **114**, 090501 (2015).
- [21] Eisert, J. et al. Quantum certification and benchmarking. *Nat. Rev. Phys.* **2**, 382–390 (2020).
- [22] Šupić, I. & Bowles, J. Self-testing of quantum systems: a review. *Quantum* **4**, 337 (2020).
- [23] Pappa, A., Chailloux, A., Wehner, S., Diamanti, E. & Kerenidis, I. Multipartite Entanglement Verification Resistant against Dishonest Parties. *Phys. Rev. Lett.* **108**, 260502 (2012).
- [24] McCutcheon, W. et al. Experimental verification of multipartite entanglement in quantum networks. *Nat. Commun.* **7**, 13251 (2016).
- [25] Šupić, I. & Hoban, M. J. Self-testing through EPR-steering. *New J. Phys.* **18**, 075006 (2016).
- [26] Gheorghiu, A., Wallden, P. & Kashefi, E. Rigidity of quantum steering and one-sided device-independent verifiable quantum computation. *New J. Phys.* **19**, 023043 (2017).
- [27] Lu, H. et al. Counting Classical Nodes in Quantum Networks. *Phys. Rev. Lett.* **124**, 180503 (2020).
- [28] Markham, D. & Krause, A. A Simple Protocol for Certifying Graph States and Applications in Quantum Networks. *Cryptography* **4**, 3 (2020).
- [29] Unnikrishnan, A. & Markham, D. Verification of graph states in an untrusted network. Preprint at <http://arxiv.org/abs/2007.13126> (2020).
- [30] Branciard, C., Cavalcanti, E. G., Walborn, S. P., Scarani, V. & Wiseman, H. M. One-sided device-independent quantum key distribution: Security, feasibility, and the connection with steering. *Phys. Rev. A* **85**, 010301(R) (2012).
- [31] Unnikrishnan, A. et al. Anonymity for Practical Quantum Networks. *Phys. Rev. Lett.* **122**, 240501 (2019).
- [32] Hahn, F., de Jong, J. & Pappa, A. Anonymous Quantum Conference Key Agreement. *PRX Quantum* **1**, 020325 (2020).
- [33] Hayashi, M. & Koshiba, T. Verifiable Quantum Secure Modulo Summation. Preprint at <http://arxiv.org/abs/1910.05976> (2019).
- [34] Wiseman, H. M., Jones, S. J. & Doherty, A. C. Steering, Entanglement, Nonlocality, and the Einstein-Podolsky-Rosen Paradox. *Phys. Rev. Lett.* **98**, 140402 (2007).
- [35] Saunders, D. J., Jones, S. J., Wiseman, H. M. & Pryde, G. J. Experimental EPR-steering using Bell-local states. *Nat. Phys.* **6**, 845–849 (2010).
- [36] Cavalcanti, D. et al. Detection of entanglement in asymmetric quantum networks and multipartite quantum steering. *Nat. Commun.* **6**, 7941 (2015).
- [37] Berta, M., Christandl, M., Colbeck, R., Renes, J. M. & Renner, R. The uncertainty principle in the presence of quantum memory. *Nat. Phys.* **6**, 659–662 (2010).
- [38] Zhu, H. Zero uncertainty states in the presence of quantum memory. *npj Quantum Inf.* **7**, 47 (2021).
- [39] Flammia, S. T. & Liu, Y.-K. Direct Fidelity Estimation from Few Pauli Measurements. *Phys. Rev. Lett.* **106**, 230501 (2011).
- [40] Hayashi, M., Matsumoto, K. & Tsuda, Y. A study of LOCC-detection of a maximally entangled state using hypothesis testing. *J. Phys. A: Math. Gen.* **39**, 14427–14446 (2006).
- [41] Hayashi, M. Group theoretical study of LOCC-detection of maximally entangled states using hypothesis testing. *New J. Phys.* **11**, 043028 (2009).
- [42] Pallister, S., Linden, N. & Montanaro, A. Optimal Verification of Entangled States with Local Measurements. *Phys. Rev. Lett.* **120**, 170502 (2018).
- [43] Zhu, H. & Hayashi, M. Efficient Verification of Pure Quantum States in the Adversarial Scenario. *Phys. Rev. Lett.* **123**, 260504 (2019).
- [44] Zhu, H. & Hayashi, M. General framework for verifying pure quantum states in the adversarial scenario. *Phys. Rev. A* **100**, 062335 (2019).
- [45] Takeuchi, Y. & Morimae, T. Verification of Many-Qubit States. *Phys. Rev. X* **8**, 021060 (2018).
- [46] Dimić, A., Šupić, I. & Dakić, B. Sample-efficient device-independent quantum state verification and certification. Preprint at <http://arxiv.org/abs/2105.05832> (2021).
- [47] Mayers, D. & Yao, A. Self Testing Quantum Apparatus, *Quantum Inf. Comput.* **4**, 273 (2004).
- [48] McKague, M., Yang, T. H. & Scarani, V. Robust self-

- testing of the singlet. *J. Phys. A: Math. Theor.* **45**, 455304 (2012).
- [49] Yang, T. H., Vértesi, T., Bancal, J.-D., Scarani, V. & Navascués, M. Robust and Versatile Black-Box Certification of Quantum Devices. *Phys. Rev. Lett.* **113**, 040401 (2014).
 - [50] Kaniewski, J. Analytic and Nearly Optimal Self-Testing Bounds for the Clauser-Horne-Shimony-Holt and Mermin Inequalities. *Phys. Rev. Lett.* **117**, 070402 (2016).
 - [51] Hayashi, M. & Hajdušek, M. Self-Guaranteed Measurement-Based Quantum Computation, *Phys. Rev. A* **97**, 052308 (2018).
 - [52] Metger, T. & Vidick, T. Self-testing of a single quantum device under computational assumptions. *Quantum* **5**, 544 (2021).
 - [53] Zhu, H. & Hayashi, M. Optimal verification and fidelity estimation of maximally entangled states. *Phys. Rev. A* **99**, 052346 (2019).
 - [54] Wang, K. & Hayashi, M. Optimal Verification of Two-Qubit Pure States. *Phys. Rev. A* **100**, 032315 (2019).
 - [55] Li, Z., Han, Y.-G. & Zhu, H. Efficient verification of bipartite pure states. *Phys. Rev. A* **100**, 032316 (2019).
 - [56] Yu, X.-D., Shang, J. & Gühne, O. Optimal verification of general bipartite pure states. *npj Quantum Inf.* **5**, 112 (2019).
 - [57] Li, Z., Han, Y.-G. & Zhu, H. Optimal Verification of Greenberger-Horne-Zeilinger States. *Phys. Rev. Appl.* **13**, 054002 (2020).
 - [58] Dangniam, N., Han, Y.-G. & Zhu, H. Optimal verification of stabilizer states. *Phys. Rev. Res.* **2**, 043323 (2020).
 - [59] Helstrom, C. W. Quantum Detection and Estimation Theory (Academic, 1976).
 - [60] Jevtic, S., Pusey, M., Jennings, D. & Rudolph, T. Quantum Steering Ellipsoids. *Phys. Rev. Lett.* **113**, 020402 (2014).
 - [61] Zhang, C. et al. Experimental Validation of Quantum Steering Ellipsoids and Tests of Volume Monogamy Relations. *Phys. Rev. Lett.* **122**, 070402 (2019).
 - [62] Wootters, W. K. Entanglement of formation of an arbitrary state of two qubits. *Phys. Rev. Lett.* **80**, 2245 (1998).
 - [63] Verstraete, F. & Verschelde, H. Fidelity of mixed states of two qubits. *Phys. Rev. A* **66**, 022307 (2002).
 - [64] Gühne, O. & Tóth, G. *Entanglement Detection*, *Phys. Rep.* **474**, 1-75 (2009).

SUPPLEMENTARY MATERIAL

In this Supplementary Material we provide rigorous proofs for the Theorems and Lemmas presented in the main text together with some auxiliary results. First, we prove several key results on the guessing probability, including Eqs. (2), (3), and Theorem 1 in the main text. Then we prove Lemma 1 and Theorem 2 after summarizing the basic properties of the guessing probability. Next, we consider the fidelity as the figure of merit and prove Theorem 3. Next, we determine the sample efficiencies of our verification protocols and explain the significance of the guessing probability threshold. Next, we compare the sample efficiency of semi-device-independent (SDI) quantum state verification (QSV) with standard QSV and device-independent (DI) QSV based on self-testing. Next, we propose a number of concrete protocols for verifying the Bell state, including protocols based on polygons and platonic solids; the properties of these protocols are discussed in detail. Finally, we establish an intimate connection between the verification of GHZ states and the verification of the Bell state, which enables us to construct efficient and even optimal protocols for verifying GHZ states. In the course of study, we introduce the concept of compatible measurements, which is of interest beyond the main focus of this work.

SUPPLEMENTARY NOTE 1: GUESSING PROBABILITY

Here we prove several key results on the guessing probability, namely, Eqs. (2), (3), and Theorem 1 in the main text.

Proof of Eq. (2). Recall that any two-qubit state has the form

$$\rho = \frac{1}{4} \left(\mathbb{I} + \mathbf{a} \cdot \boldsymbol{\sigma} \otimes \mathbb{I} + \mathbb{I} \otimes \mathbf{b} \cdot \boldsymbol{\sigma} + \sum_{j,k} T_{j,k} \sigma_j \otimes \sigma_k \right). \quad (\text{S1})$$

After Alice performs the projective measurement $\mathbf{r} \cdot \boldsymbol{\sigma}$, the unnormalized reduced states of Bob associated with the two outcomes read

$$\rho_{\pm} = \text{tr}_A(\rho P_{\pm}) = \frac{1}{4} \left(\mathbb{I} \pm \mathbf{a} \cdot \mathbf{r} \mathbb{I} + \mathbf{b} \cdot \boldsymbol{\sigma} \pm \sum_{j,k} T_{j,k} r_j \sigma_k \right), \quad (\text{S2})$$

which implies that

$$\rho_+ - \rho_- = \frac{1}{2} \left(\mathbf{a} \cdot \mathbf{r} \mathbb{I} + \sum_{j,k} T_{j,k} r_j \sigma_k \right). \quad (\text{S3})$$

Therefore,

$$\begin{aligned} \gamma(\rho, \mathbf{r}) &= \frac{1}{2} + \frac{1}{2} \|\rho_+ - \rho_-\|_1 \\ &= \frac{1}{2} + \frac{1}{4} \left\| \mathbf{a} \cdot \mathbf{r} \mathbb{I} + \sum_{j,k} T_{j,k} r_j \sigma_k \right\|_1 \\ &= \frac{1}{2} (1 + \max\{|\mathbf{a} \cdot \mathbf{r}|, \|T^T \mathbf{r}\|\}). \end{aligned} \quad (\text{S4})$$

If ρ is pure, then $\rho_+ - \rho_-$ has at most one positive eigenvalue and one negative eigenvalue. So $|\mathbf{a} \cdot \mathbf{r}| \leq \|T^T \mathbf{r}\|$ and

$$\gamma(\rho, \mathbf{r}) = \frac{1}{2} (1 + \|T^T \mathbf{r}\|), \quad (\text{S5})$$

which confirms Eq. (2). \square

Proof of Eq. (3). If ρ is a pure state with concurrence C , then its correlation matrix T has three singular values $1, C, C$, and so does T^T . Accordingly, TT^T has three eigenvalues $1, C^2, C^2$. The semi-major axis \mathbf{v} of the correlation ellipsoid happens to be an eigenvector of TT^T with eigenvalue 1. Therefore,

$$\begin{aligned} \|\sqrt{TT^T} \mathbf{r}\|^2 &= \|T^T \mathbf{r}\|^2 = \mathbf{r}^T TT^T \mathbf{r} \\ &= (\mathbf{r} \cdot \mathbf{v})^2 + C^2 [1 - (\mathbf{r} \cdot \mathbf{v})^2] = C^2 + (1 - C^2)(\mathbf{r} \cdot \mathbf{v})^2, \end{aligned} \quad (\text{S6})$$

which implies Eq. (3). \square

Proof of Theorem 1. Given any unit vector \mathbf{v} on the Bloch sphere, there exists a two-qubit pure state ρ with concurrence C and correlation matrix T such that \mathbf{v} is an eigenvector of TT^T associated with the eigenvalue 1. In other words, the semi-major axis of the correlation ellipsoid of ρ can be chosen to coincide with \mathbf{v} . So Theorem 1 follows from Eqs. (2) and (3) in the main text. \square

Theorem 1 implies that

$$\begin{aligned} \gamma_2(C, \mu) &= \max_{\rho} \{\gamma(\rho, \mu) | C(\rho) \leq C\} \\ &= \max_{\rho} \{\gamma(\rho, \mu) | C(\rho) = C\}, \end{aligned} \quad (\text{S7})$$

where both maximizations are taken over two-qubit pure states. This result corroborates the intuition that the maximum guessing probability is nondecreasing with the concurrence.

SUPPLEMENTARY NOTE 2: BASIC PROPERTIES OF THE GUESSING PROBABILITY

Here we summarize the basic properties of the guessing probability $\gamma_2(C, \mu)$ and the function $g(C, \mu)$.

Lemma S1. Suppose $0 \leq C \leq 1$; then $g(C, \mu)$ is nondecreasing in C ; in addition, $g(C, \mu)$ is convex in C and μ , respectively, that is,

$$g(p_1 C_1 + p_2 C_2, \mu) \leq p_1 g(C_1, \mu) + p_2 g(C_2, \mu), \quad (\text{S8})$$

$$g(C, p_1 \mu_1 + p_2 \mu_2) \leq p_1 g(C, \mu_1) + p_2 g(C, \mu_2), \quad (\text{S9})$$

where $p_1, p_2 \geq 0$, $p_1 + p_2 = 1$, $0 \leq C_1, C_2 \leq 1$, and μ_1, μ_2 are two probability distributions on the Bloch sphere. Similarly, $\gamma_2(C, \mu)$ is nondecreasing in C and is convex in C and μ , respectively.

Lemma S1 follows from Eqs. (6) and (5) in Theorem 1. The monotonicity of $\gamma_2(C, \mu)$ is also clear from its definition.

If μ_1 and μ_2 can be turned into each other by an orthogonal transformation, then $g(C, \mu_1) = g(C, \mu_2)$, so

$$g(C, p_1 \mu_1 + p_2 \mu_2) \leq g(C, \mu_1). \quad (\text{S10})$$

Therefore, $g(C, \mu)$ for given C is minimized when μ is the uniform distribution on the Bloch sphere.

The verification matrix of the distribution μ is defined as

$$\Xi(\mu) := \int d\mu(\mathbf{r}) \mathbf{r} \mathbf{r}^T, \quad (\text{S11})$$

which is a 3×3 positive-semidefinite matrix with trace 1, that is, $\text{tr}[\Xi(\mu)] = 1$. The operator norm (the largest eigenvalue) of $\Xi(\mu)$ is bounded from below by $1/3$, that is, $\|\Xi(\mu)\| \geq 1/3$. The distribution μ and the corresponding protocol are *balanced* if $\Xi(\mu)$ is proportional to the identity matrix, in which case the lower bound $\|\Xi(\mu)\| \geq 1/3$ is saturated.

As we shall see shortly, the properties of $g(C, \mu)$ is closely tied to the verification matrix $\Xi(\mu)$. For example, an upper bound for $g(C, \mu)$ can be constructed from $\Xi(\mu)$, as shown in the following lemma.

Lemma S2. Suppose $0 \leq C \leq 1$; then

$$g(C, \mu) \leq \sqrt{C^2 + (1 - C^2)\|\Xi(\mu)\|}. \quad (\text{S12})$$

The inequality is saturated if there exists a unit vector \mathbf{v} in the eigenspace of $\Xi(\mu)$ associated with the largest eigenvalue and $|\mathbf{r} \cdot \mathbf{v}|$ is a constant in the support of μ except for a set of measure zero. Any such unit vector, if it exists, represents an intelligent direction.

Proof of Lemma S2. Let \mathbf{v} be an arbitrary unit vector in dimension 3. The upper bound in Eq. (S12) follows from Eq. (6) in the main text and the following equation

$$\begin{aligned} & \int d\mu(\mathbf{r}) \sqrt{C^2 + (1 - C^2)(\mathbf{r} \cdot \mathbf{v})^2} \\ & \leq \sqrt{C^2 + (1 - C^2) \int d\mu(\mathbf{r}) (\mathbf{r} \cdot \mathbf{v})^2} \\ & = \sqrt{C^2 + (1 - C^2) \mathbf{v}^T \Xi \mathbf{v}} \\ & \leq \sqrt{C^2 + (1 - C^2) \|\Xi\|}, \end{aligned} \quad (\text{S13})$$

where Ξ is an abbreviation of $\Xi(\mu)$. Here the first inequality is due to the concavity of the square-root function and is saturated iff $|\mathbf{r} \cdot \mathbf{v}|$ is a constant in the support of μ except for a set of measure zero; the second inequality is saturated iff \mathbf{v} is an eigenvector of Ξ with the largest eigenvalue $\|\Xi\|$. So the inequality in Eq. (S12) is saturated iff there exists a unit vector \mathbf{v} that belongs to the eigenspace of Ξ associated with the largest eigenvalue and $|\mathbf{r} \cdot \mathbf{v}|$ is a constant in the support of μ except for a set of measure zero. In addition, any such unit vector, if it exists, represents an intelligent direction. \square

By contrast, a lower bound for $g(C, \mu)$ can be constructed by choosing \mathbf{v} as an eigenvector of $\Xi(\mu)$ associated with the largest eigenvalue. Alternative lower bounds are presented in the following lemma.

Lemma S3. Suppose $0 \leq C \leq 1$; then

$$g(C, \mu) \geq \|\Xi\| + (1 - \|\Xi\|)C \geq \frac{1 + 2C}{3} \geq C, \quad (\text{S14})$$

$$\gamma_2(C, \mu) \geq \frac{1 + \|\Xi\| + (1 - \|\Xi\|)C}{2} \geq \frac{2 + C}{3} \geq C. \quad (\text{S15})$$

Proof. Equation (S14) can be derived as follows,

$$\begin{aligned} g(C, \mu) &= \max_{\mathbf{v}} \int d\mu(\mathbf{r}) \sqrt{C^2 + (1 - C^2)(\mathbf{r} \cdot \mathbf{v})^2} \\ &\geq \max_{\mathbf{v}} [(1 - \mathbf{v}^T \Xi \mathbf{v})C + \mathbf{v}^T \Xi \mathbf{v}] \\ &= (1 - \|\Xi\|)C + \|\Xi\| \geq \frac{1 + 2C}{3} \geq C. \end{aligned} \quad (\text{S16})$$

Here the first inequality follows from the concavity of the square-root function and the constraint $0 \leq (\mathbf{r} \cdot \mathbf{v})^2 \leq 1$; the second inequality follows from the facts $\|\Xi\| \geq 1/3$ and $0 \leq C \leq 1$.

Equation (S15) follows from Eq. (S14) and the equality $\gamma_2(C, \mu) = [1 + g(C, \mu)]/2$ in Eq. (5) in the main text. \square

The bound in Eq. (S14) is nearly tight when $C \rightarrow 1$. To see this point, note that

$$\begin{aligned} & \int d\mu(\mathbf{r}) \sqrt{C^2 + (1 - C^2)(\mathbf{r} \cdot \mathbf{v})^2} \\ & \approx \int d\mu(\mathbf{r}) \left\{ 1 - \frac{1}{2} [1 - (\mathbf{r} \cdot \mathbf{v})^2] (1 - C^2) \right\} \\ & = 1 - \frac{1}{2} (1 - \mathbf{v}^T \Xi \mathbf{v}) (1 - C^2) \approx 1 - (1 - \mathbf{v}^T \Xi \mathbf{v}) (1 - C) \\ & = [1 - \mathbf{v}^T \Xi \mathbf{v}] C + \mathbf{v}^T \Xi \mathbf{v}, \end{aligned} \quad (\text{S17})$$

where we have kept the first-order approximation in $1 - C$. This equation implies that

$$g(C, \mu) \approx \|\Xi\| + (1 - \|\Xi\|)C, \quad (\text{S18})$$

so the bound in Eq. (S14) is nearly tight when $C \rightarrow 1$. In the limit $C \rightarrow 1$, Eq. (S18) implies that $g(C, \mu)$ is minimized when $\|\Xi\| = 1/3$, that is, $\Xi = \mathbb{I}/3$, so that the verification protocol is balanced.

Lemma S4. Suppose $0 \leq C_1 \leq C_2 \leq 1$; then

$$g(C_2, \mu) - g(C_1, \mu) \leq \frac{2}{3}(C_2 - C_1). \quad (\text{S19})$$

Proof. When $C_2 = 1$, we have $g(C_2) = 1$, so Eq. (S19) reduces to the equation

$$1 - g(C_1, \mu) \leq \frac{2}{3}(1 - C_1) \quad (\text{S20})$$

and so follows from Eq. (S14).

When $0 \leq C_1 \leq C_2 < 1$, Eq. (S19) can be derived as follows

$$\begin{aligned} g(C_2, \mu) - g(C_1, \mu) &\leq \frac{C_2 - C_1}{1 - C_1} [g(C = 1, \mu) - g(C_1, \mu)] \\ &= \frac{C_2 - C_1}{1 - C_1} [1 - g(C_1, \mu)] \leq \frac{C_2 - C_1}{1 - C_1} \times \frac{2}{3}(1 - C_1) \\ &= \frac{2}{3}(C_2 - C_1). \end{aligned} \quad (\text{S21})$$

Here the first inequality follows from the facts that $g(C, \mu)$ is nondecreasing and convex in C ; the second inequality follows from Eq. (S20). \square

Lemma S5. Suppose $0 \leq C \leq p \leq 1$ and $p > 0$; then

$$pg\left(\frac{C}{p}, \mu\right) \leq g(C, \mu), \quad (\text{S22})$$

$$p\gamma_2\left(\frac{C}{p}, \mu\right) \leq \gamma_2(C, \mu). \quad (\text{S23})$$

Proof. According to Lemma S4, we have

$$g\left(\frac{C}{p}, \mu\right) \leq g(C, \mu) + \frac{2}{3}\left(\frac{C}{p} - C\right), \quad (\text{S24})$$

so

$$\begin{aligned} pg\left(\frac{C}{p}, \mu\right) - g(C, \mu) &\leq -(1 - p)g(C, \mu) + \frac{2}{3}(1 - p)C \\ &= -(1 - p)\left[g(C, \mu) - \frac{2}{3}C\right] \leq -\frac{1 - p}{3}, \end{aligned} \quad (\text{S25})$$

which implies Eq. (S22). Here the last inequality follows from Lemma S3.

Equation (S23) follows from Eq. (S22) and the equality $\gamma_2(C, \mu) = [1 + g(C, \mu)]/2$ in Eq. (5) in the main text. \square

Lemma S6. Suppose the strategy μ satisfies

$$\int d\mu(\mathbf{r})\mathbf{r} = 0. \quad (\text{S26})$$

Then $g^*(\mu)$ defined in Eq. (7) in the main text can be expressed as

$$g^*(\mu) = 2 \max_R \left| \int_R d\mu(\mathbf{r})\mathbf{r} \right| = 2 \max_{\mathbf{v}} \left| \int_{\mathbf{r} \cdot \mathbf{v} \geq 0} d\mu(\mathbf{r})\mathbf{r} \right|, \quad (\text{S27})$$

where the first maximization is over all measurable subsets of the Bloch sphere, and the second maximization is over all unit vectors on the Bloch sphere. In addition, \mathbf{v} is an intelligent direction at $C = 0$ iff it satisfies the following two conditions,

$$\mathbf{v} \parallel \int_{\mathbf{r} \cdot \mathbf{v} \geq 0} d\mu(\mathbf{r})\mathbf{r}, \quad 2 \left| \int_{\mathbf{r} \cdot \mathbf{v} \geq 0} d\mu(\mathbf{r})\mathbf{r} \right| = g^*(\mu). \quad (\text{S28})$$

Proof. Let R be any measurable subset of the Bloch sphere and \bar{R} its complement; then we have

$$\int_R d\mu(\mathbf{r})\mathbf{r} = - \int_{\bar{R}} d\mu(\mathbf{r})\mathbf{r} \quad (\text{S29})$$

by the assumption Eq. (S26). Therefore,

$$\begin{aligned} \int d\mu(\mathbf{r})|\mathbf{r} \cdot \mathbf{v}| &= \int_{\mathbf{r} \cdot \mathbf{v} \geq 0} d\mu(\mathbf{r})\mathbf{r} \cdot \mathbf{v} - \int_{\mathbf{r} \cdot \mathbf{v} < 0} d\mu(\mathbf{r})\mathbf{r} \cdot \mathbf{v} \\ &= 2\mathbf{v} \cdot \int_{\mathbf{r} \cdot \mathbf{v} \geq 0} d\mu(\mathbf{r})\mathbf{r} \geq 2\mathbf{v} \cdot \int_R d\mu(\mathbf{r})\mathbf{r}; \end{aligned} \quad (\text{S30})$$

here the inequality is saturated if R is the region determined by the inequality $\mathbf{r} \cdot \mathbf{v} \geq 0$. It follows that

$$\int d\mu(\mathbf{r})|\mathbf{r} \cdot \mathbf{v}| = 2 \max_R \left[\mathbf{v} \cdot \int_R d\mu(\mathbf{r})\mathbf{r} \right]. \quad (\text{S31})$$

By plugging Eq. (S31) into Eq. (7) in the main text we obtain

$$\begin{aligned} g^*(\mu) &= \max_{\mathbf{v}} \int d\mu(\mathbf{r})|\mathbf{r} \cdot \mathbf{v}| = 2 \max_{\mathbf{v}, R} \left[\mathbf{v} \cdot \int_R d\mu(\mathbf{r})\mathbf{r} \right] \\ &= 2 \max_R \left| \int_R d\mu(\mathbf{r})\mathbf{r} \right|, \end{aligned} \quad (\text{S32})$$

which confirms the first equality in Eq. (S27). The second equality in Eq. (S27) follows from the equation below,

$$\begin{aligned} 2 \max_{\mathbf{v}} \left| \int_{\mathbf{r} \cdot \mathbf{v} \geq 0} d\mu(\mathbf{r})\mathbf{r} \right| &\leq 2 \max_R \left| \int_R d\mu(\mathbf{r})\mathbf{r} \right| = g^*(\mu) \\ &= \max_{\mathbf{v}} \int d\mu(\mathbf{r})|\mathbf{r} \cdot \mathbf{v}| = 2 \max_{\mathbf{v}} \mathbf{v} \cdot \int_{\mathbf{r} \cdot \mathbf{v} \geq 0} d\mu(\mathbf{r})\mathbf{r} \\ &\leq 2 \max_{\mathbf{v}} \left| \int_{\mathbf{r} \cdot \mathbf{v} \geq 0} d\mu(\mathbf{r})\mathbf{r} \right|. \end{aligned} \quad (\text{S33})$$

According to (S30), \mathbf{v} is an intelligent direction iff

$$2\mathbf{v} \cdot \int_{\mathbf{r} \cdot \mathbf{v} \geq 0} d\mu(\mathbf{r})\mathbf{r} = g^*(\mu). \quad (\text{S34})$$

In view of Eq. (S27), this condition holds iff the conditions in Eq. (S28) hold. \square

SUPPLEMENTARY NOTE 3: PROOF OF LEMMA 1

Here we prove Lemma 1 presented in the main text, which shows that Bob cannot increase the guessing probability by preparing a higher-dimensional state ρ whose

local support for Alice is not contained in the local support of the target Bell state.

Let $\rho_A = \text{tr}_B(\rho)$ and let

$$P_A = |0\rangle\langle 0| + |1\rangle\langle 1| \quad (\text{S35})$$

be the projector onto the local support of the target Bell state. Before proving Lemma 1, it is instructive to give formal mathematical definitions of $\gamma_2(C, \mu)$ and $\gamma(C, \mu)$:

$$\gamma_2(C, \mu) = \max_{\rho} \{ \gamma(\rho, \mu) | C(\rho) \leq C, \rho^2 = \rho, P_A \rho_A = \rho_A \}, \quad (\text{S36})$$

$$\gamma(C, \mu) = \max_{\rho} \{ \gamma(\rho, \mu) | C(\rho) \leq C, \rho^2 = \rho \}. \quad (\text{S37})$$

Here the constraint $\rho^2 = \rho$ means ρ is a pure state, while the constraint $P_A \rho_A = \rho_A$ means ρ_A is supported in the support of P_A (the local support of the target Bell state). By definition we have

$$\gamma(C, \mu) \geq \gamma_2(C, \mu). \quad (\text{S38})$$

To prove the equality $\gamma(C, \mu) = \gamma_2(C, \mu)$, it suffices to derive the opposite inequality.

Proof of Lemma 1. If Alice performs the projective measurement $\{P_A, \mathbb{I} - P_A\}$ on the state ρ , then the probability of obtaining the first outcome is $q = \text{tr}[(P_A \otimes \mathbb{I}_B)\rho]$. When $q > 0$, after obtaining this outcome, the state ρ turns into

$$\rho' = \frac{1}{q} (P_A \otimes \mathbb{I}_B) \rho (P_A \otimes \mathbb{I}_B). \quad (\text{S39})$$

Note that $\text{tr}_B(\rho')$ is supported in the support of P_A . In addition, the concurrence of ρ' obeys the upper bound

$$C(\rho') \leq \min\{C(\rho)/q, 1\}. \quad (\text{S40})$$

When $q > 0$ and $C(\rho) \leq q$, the guessing probability of Bob satisfies

$$\begin{aligned} \gamma(\rho, \mu) &= q\gamma(\rho', \mu) \leq q\gamma_2(C(\rho'), \mu) \leq q\gamma_2(C(\rho)/q, \mu) \\ &\leq \gamma_2(C(\rho), \mu). \end{aligned} \quad (\text{S41})$$

Here the first inequality follows from the definition of $\gamma_2(C, \mu)$; the second inequality follows from the inequality $C(\rho') \leq C(\rho)/q$ and the monotonicity of $\gamma_2(C, \mu)$ in C (cf. Lemma S1); the third inequality follows from Eq. (S23) in Lemma S5.

When $0 < q \leq C(\rho) \leq 1$, the guessing probability of Bob satisfies

$$\gamma(\rho, \mu) = q\gamma(\rho', \mu) \leq q \leq C(\rho) \leq \gamma_2(C(\rho), \mu), \quad (\text{S42})$$

where the first inequality follows from the fact that $\gamma_2(C, \mu) \leq 1$ and the last inequality follows from Eq. (S15) in Lemma S3.

Equations (S41) and (S42) together imply that

$$\gamma(\rho, \mu) \leq \gamma_2(C(\rho), \mu). \quad (\text{S43})$$

Note that this equation holds even if $q = 0$ in which case $\gamma(\rho, \mu) = 0$. As a corollary of Eq. (S43), we can deduce

$$\begin{aligned} \gamma(C, \mu) &= \max_{\rho} \{ \gamma(\rho, \mu) | C(\rho) \leq C, \rho^2 = \rho \} \\ &\leq \max_{\rho} \{ \gamma_2(C(\rho), \mu) | C(\rho) \leq C \} = \gamma_2(C, \mu). \end{aligned} \quad (\text{S44})$$

Here the last equality follows from the monotonicity of $\gamma_2(C, \mu)$ in C (cf. Lemma S1). Since $\gamma(C, \mu) \geq \gamma_2(C, \mu)$ by definition, Eq. (S44) implies that $\gamma(C, \mu) = \gamma_2(C, \mu)$ for $0 \leq C \leq 1$, which confirms Lemma 1. \square

SUPPLEMENTARY NOTE 4: PROOF OF THEOREM 2

Here we prove Theorem 2 presented in the main text, which determines the maximum guessing probability for mixed states.

Proof of Theorem 2. The third equality in Eq. (10) in the theorem follows from Eq. (8) in the main text and the equality $\gamma^*(\mu) = \gamma_2^*(\mu)$.

The second equality in Eq. (10) is equivalent to the following equality

$$\hat{\gamma}_2(C, \mu) = (1 - C)\gamma_2^*(\mu) + C \quad (\text{S45})$$

given that $\gamma^*(\mu) = \gamma_2^*(\mu)$. Suppose ρ is the state prepared by Bob and $\rho_A = \text{tr}_B(\rho)$ is supported in the support of P_A defined in Eq. (S35). Let $\rho = \sum_j q_j \rho_j$ be any convex decomposition of ρ into pure states such that $C(\rho) = \sum_j q_j C_j$, where $C_j = C(\rho_j)$ is the concurrence of ρ_j . Note that $\text{tr}_B(\rho_j)$ is supported in the support of P_A and $C_j \leq 1$ for each j . Then the guessing probability of Bob satisfies

$$\begin{aligned} \hat{\gamma}(\rho, \mu) &\leq \sum_j q_j \gamma(\rho_j, \mu) \leq \sum_j q_j \gamma_2(C_j, \mu) \\ &\leq [1 - C(\rho)]\gamma_2(0, \mu) + C(\rho)\gamma_2(1, \mu) \\ &= [1 - C(\rho)]\gamma_2^*(\mu) + C(\rho). \end{aligned} \quad (\text{S46})$$

Here the third inequality follows from the convexity of $\gamma_2(C, \mu)$ in C (cf. Lemma S1); the last equality follows from the facts that $\gamma_2(1, \mu) = 1$ and $\gamma_2^*(\mu) = \gamma_2(0, \mu)$. As an implication of Eq. (S46), we have

$$\begin{aligned} \hat{\gamma}_2(C, \mu) &= \max_{\rho} \{ \gamma(\rho, \mu) | C(\rho) \leq C, P_A \rho_A = \rho_A \} \\ &\leq \max_{\rho} \{ [1 - C(\rho)]\gamma_2^*(\mu) + C(\rho) | C(\rho) \leq C \} \\ &= (1 - C)\gamma_2^*(\mu) + C. \end{aligned} \quad (\text{S47})$$

To prove the second equality in Eq. (10), it remains to prove the opposite inequality to Eq. (S47), that is,

$$\hat{\gamma}_2(C, \mu) \geq (1 - C)\gamma_2^*(\mu) + C. \quad (\text{S48})$$

Let ρ_1 be a pure product state such that $\text{tr}_B(\rho_1)$ is supported in the support of P_A and that $\gamma(\rho_1, \mu) = \gamma_2^*(\mu)$.

Let ρ_2 be a Bell state such that $\text{tr}_B(\rho_2)$ is supported in the support of P_A and that the support of $\text{tr}_A \rho_2$ is orthogonal to that of $\text{tr}_A \rho_1$. Then $\gamma(\rho_2, \mu) = 1$ and $C(\rho_2) = 1$. Let $\rho = (1-p)\rho_1 + p\rho_2$ with $0 \leq p \leq 1$; then

$$C(\rho) = (1-p)C(\rho_1) + pC(\rho_2) = p, \quad (\text{S49})$$

$$\begin{aligned} \gamma(\rho, \mu) &= (1-p)\gamma(\rho_1, \mu) + p\gamma(\rho_2, \mu) \\ &= (1-p)\gamma_2^*(\mu) + p. \end{aligned} \quad (\text{S50})$$

By setting $p = C$, we can deduce Eq. (S48), which implies Eq. (S45) and the second equality in Eq. (10).

Finally, let us prove the first equality in Eq. (10). Since $\hat{\gamma}(C, \mu) \geq \hat{\gamma}_2(C, \mu)$ by definition, it remains to prove the opposite inequality.

Suppose ρ is the state prepared by Bob; here the support of $\rho_A = \text{tr}_B(\rho)$ is not restricted in contrast to the above discussions. Let $q = \text{tr}[(P_A \otimes \mathbb{I}_B)\rho]$ and

$$\rho' = \frac{1}{q}(P_A \otimes \mathbb{I}_B)\rho(P_A \otimes \mathbb{I}_B), \quad q > 0; \quad (\text{S51})$$

then $C(\rho') \leq \min\{C(\rho)/q, 1\}$. When $q > 0$ and $C(\rho) \leq q$, the guessing probability of Bob satisfies

$$\begin{aligned} \gamma(\rho, \mu) &= q\gamma(\rho', \mu) \leq q\hat{\gamma}_2(C(\rho'), \mu) \leq q\hat{\gamma}_2(C(\rho)/q, \mu) \\ &\leq \hat{\gamma}_2(C(\rho), \mu). \end{aligned} \quad (\text{S52})$$

Here the first inequality follows from the definition of $\hat{\gamma}_2(C, \mu)$; the second inequality follows from the inequality $C(\rho') \leq C(\rho)/q$ and the monotonicity of $\hat{\gamma}_2(C, \mu)$ in C according to Eq. (S45); the third inequality also follows from Eq. (S45).

When $0 < q \leq C(\rho) \leq 1$, the guessing probability of Bob satisfies

$$\gamma(\rho, \mu) = q\gamma(\rho', \mu) \leq q \leq C(\rho) \leq \hat{\gamma}_2(C(\rho), \mu), \quad (\text{S53})$$

where the last inequality follows from Eq. (S45) again.

Equations (S52) and (S53) together imply that

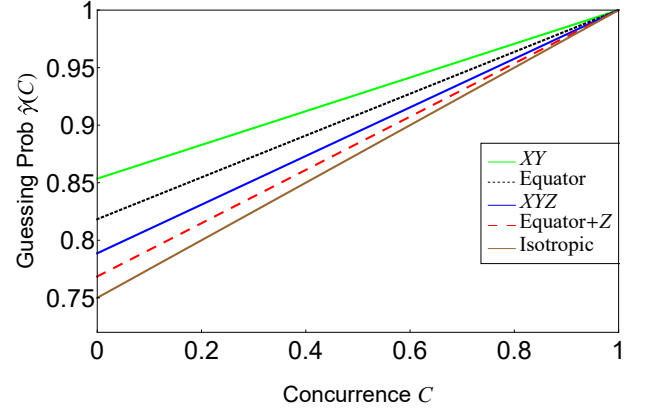
$$\gamma(\rho, \mu) \leq \hat{\gamma}_2(C(\rho), \mu). \quad (\text{S54})$$

This equation holds even when $q = 0$, in which case we have $\gamma(\rho, \mu) = 0$. As a corollary of Eq. (S54) we can deduce

$$\begin{aligned} \hat{\gamma}(C, \mu) &= \max_{\rho} \{\gamma(\rho, \mu) | C(\rho) \leq C\} \\ &\leq \max_{\rho} \{\hat{\gamma}_2(C(\rho), \mu) | C(\rho) \leq C\} = \hat{\gamma}_2(C, \mu). \end{aligned} \quad (\text{S55})$$

Here the last equality follows from the monotonicity of $\hat{\gamma}_2(C, \mu)$ in C by Eq. (S45). Given the opposite inequality by definition, we conclude that $\hat{\gamma}(C, \mu) = \hat{\gamma}_2(C, \mu)$, which completes the proof of Eq. (10) and Theorem 2. \square

To complement Fig. 2 in the main text, the relation between the guessing probability and concurrence in the mixed-state scenario is illustrated in Supplementary Figure 1.



Supplementary Figure 1. The guessing probability $\hat{\gamma}(C) = \hat{\gamma}_2(C)$ as a function of the concurrence C in the mixed-state scenario and for various verification protocols of the Bell state. Here the XY protocol and isotropic protocol are introduced in the main text, while other protocols are proposed in Supplementary Note 9.

SUPPLEMENTARY NOTE 5: FIDELITY AS THE FIGURE OF MERIT

Here we discuss in more details the properties of the guessing probabilities $\gamma_2^F(F, \mu)$ and $\gamma^F(F, \mu)$ and then prove Theorem 3 presented in the main text.

To start with we give formal mathematical definitions of $\gamma_2^F(F, \mu)$ and $\gamma^F(F, \mu)$:

$$\gamma_2^F(F, \mu) = \max_{\rho} \{\gamma(\rho, \mu) | F_B(\rho) \leq F, \rho^2 = \rho, P_A \rho_A = \rho_A\}, \quad (\text{S56})$$

$$\gamma^F(F, \mu) = \max_{\rho} \{\gamma(\rho, \mu) | F_B(\rho) \leq F, \rho^2 = \rho\}, \quad (\text{S57})$$

where $\rho_A = \text{tr}_B(\rho)$ and P_A is the projector onto the local support of the target Bell state as defined in Eq. (S35). Note that $F_B(\rho) \geq 1/2$ for any two-qubit pure state ρ that satisfies $P_A \rho = \rho$, so $\gamma_2^F(F, \mu)$ is defined only when $1/2 \leq F \leq 1$, while $\gamma^F(F, \mu)$ is defined for $0 \leq F \leq 1$.

Auxiliary results

Lemma S7. Suppose $1/2 \leq F \leq 1$; then

$$\gamma_2^F(F, \mu) = \gamma_2(2F - 1, \mu) = \frac{1}{2} + \frac{1}{2}g(2F - 1, \mu) \quad (\text{S58})$$

$$= \frac{1}{2} + \frac{1}{2} \max_{\mathbf{v}} \int d\mu(\mathbf{r}) \sqrt{(2F - 1)^2 + 4F(1 - F)(\mathbf{r} \cdot \mathbf{v})^2}. \quad (\text{S59})$$

Lemma S7 in particular implies that

$$\gamma_2^F(1/2, \mu) = \gamma_2(0, \mu) = \gamma^*(\mu) = \frac{1}{2} + \frac{1}{2}g^*(\mu), \quad (\text{S60})$$

$$\gamma_2^F(1, \mu) = \gamma_2(1, \mu) = \frac{1}{2} + \frac{1}{2}g(1, \mu) = 1. \quad (\text{S61})$$

Proof. If ρ is a pure state that satisfies the condition $P_A \rho_A = \rho_A$, then ρ is a two-qubit state and has the form in Eq. (S1). In addition, we have

$$F_B(\rho) = \frac{1 + \|T\|_1}{4} = \frac{1 + C}{2} \geq \frac{1}{2}, \quad (\text{S62})$$

where T is the correlation matrix appearing in Eq. (S1) and $\|T\|_1 = \text{tr} \sqrt{TT^\top}$. This equation implies Eq. (S58) in Lemma S7. Equation (S59) follows from Eq. (S58) above and Theorem 1 in the main text. \square

Lemma S8. *The guessing probability $\gamma_2^F(F, \mu)$ is nondecreasing in F for $1/2 \leq F \leq 1$; in addition, $\gamma_2^F(F, \mu)$ is convex in F and μ , respectively.*

Lemma S9. *Suppose $1/2 \leq F \leq 1$. Then*

$$\gamma_2^F(F, \mu) \geq \|\Xi\| + (1 - \|\Xi\|)F \geq \frac{1 + 2F}{3} \geq F, \quad (\text{S63})$$

where $\Xi = \Xi(\mu)$ is the verification matrix defined in Eq. (S11).

Lemma S8 follows from Lemmas S1 and S7. Lemma S9 follows from Lemmas S3 and S7

Lemma S10. *Suppose $0 < F \leq 1$. Then $q\gamma_2^F(F/q, \mu)$ is nondecreasing in q for $F \leq q \leq \min\{1, 2F\}$.*

Proof of Lemma S10. When $F = 1$, Lemma S10 holds trivially since q can only take on the value 1. To prove Lemma S10 when $0 < F < 1$, it suffices to prove the following inequality

$$q_1 \gamma_2^F\left(\frac{F}{q_1}, \mu\right) \leq q_2 \gamma_2^F\left(\frac{F}{q_2}, \mu\right) \quad (\text{S64})$$

for $F \leq q_1 < q_2 \leq \min\{1, 2F\}$.

Let

$$x = \frac{q_2(q_1 - F)}{q_1(q_2 - F)}, \quad (\text{S65})$$

then $0 \leq x < 1$ and

$$\frac{F}{q_1} = x \frac{F}{q_2} + 1 - x, \quad (\text{S66})$$

which implies that

$$\gamma_2^F\left(\frac{F}{q_1}, \mu\right) \leq x \gamma_2^F\left(\frac{F}{q_2}, \mu\right) + 1 - x, \quad (\text{S67})$$

given that $\gamma_2^F(F, \mu)$ is convex in F and $\gamma_2^F(F = 1, \mu) = 1$. As a consequence, we have

$$\begin{aligned} q_1 \gamma_2^F\left(\frac{F}{q_1}, \mu\right) &\leq q_1 x \gamma_2^F\left(\frac{F}{q_2}, \mu\right) + q_1(1 - x) \\ &= \frac{(q_1 - F)q_2}{(q_2 - F)} \gamma_2^F\left(\frac{F}{q_2}, \mu\right) + \frac{(q_2 - q_1)q_2}{(q_2 - F)} \frac{F}{q_2} \\ &\leq \frac{(q_1 - F)q_2}{(q_2 - F)} \gamma_2^F\left(\frac{F}{q_2}, \mu\right) + \frac{(q_2 - q_1)q_2}{(q_2 - F)} \gamma_2^F\left(\frac{F}{q_2}, \mu\right) \\ &= q_2 \gamma_2^F\left(\frac{F}{q_2}, \mu\right), \end{aligned} \quad (\text{S68})$$

which confirms Eq. (S64) and implies Lemma S10. Here the second inequality follows from Eq. (S63). \square

Lemma S11. *Suppose ρ is a bipartite state shared between Alice and Bob. Then*

$$\gamma(\rho, \mu) \leq \begin{cases} 2F_B(\rho) \gamma_2^F(1/2, \mu) & 0 \leq F_B(\rho) \leq 1/2, \\ \gamma_2^F(F_B(\rho), \mu) & 1/2 \leq F_B(\rho) \leq 1. \end{cases} \quad (\text{S69})$$

Proof of Lemma S11. Let $\rho_A = \text{tr}_B(\rho)$, $q = \text{tr}(P_A \rho_A)$, and

$$\rho' = \frac{1}{q}(P_A \otimes \mathbb{I}_B) \rho (P_A \otimes \mathbb{I}_B), \quad q > 0. \quad (\text{S70})$$

If $q = 0$, then

$$F_B(\rho) = 0, \quad \gamma(\rho, \mu) = 0. \quad (\text{S71})$$

If $0 < q \leq 1$, then $\text{tr}_B(\rho')$ is supported in the support of P_A . In addition, we have

$$F_B(\rho) = q F_B(\rho') \geq \frac{q}{2}, \quad \gamma(\rho, \mu) = q \gamma(\rho', \mu), \quad (\text{S72})$$

where the inequality is due to the fact that $F_B(\rho') \geq 1/2$ since ρ' is a two-qubit pure state with the same local support for Alice as the target Bell state.

If $F_B(\rho) = 0$, then $q = 0$ and $\gamma(\rho, \mu) = 0$, so Eq. (S69) holds.

If $F_B(\rho) > 0$, then $q > 0$, and Eq. (S72) implies that

$$\begin{aligned} \gamma(\rho, \mu) &= q \gamma(\rho', \mu) \leq q \gamma_2^F(F_B(\rho'), \mu) = q \gamma_2^F(F_B(\rho)/q, \mu) \\ &\leq \begin{cases} 2F_B(\rho) \gamma_2^F(1/2, \mu) & 0 \leq F_B(\rho) \leq 1/2, \\ \gamma_2^F(F_B(\rho), \mu) & 1/2 \leq F_B(\rho) \leq 1. \end{cases} \end{aligned} \quad (\text{S73})$$

so Eq. (S69) still holds. Here the first inequality follows from the definition of the guessing probability $\gamma_2^F(F, \mu)$, and the last inequality follows from Lemma S10 together with the constraint $F_B(\rho) \leq q \leq \min\{1, 2F_B(\rho)\}$, given that $F_B(\rho') \geq 1/2$. \square

Proof of Theorem 3

Proof of Theorem 3. First let us consider Eq. (12) in the theorem. The equality $\gamma_2^F(F, \mu) = \gamma_2(2F - 1, \mu)$ follows from the fact that $F_B(\rho) = [1 + C(\rho)]/2$ for any two-qubit pure state that satisfies $P_A \rho = \rho$ (cf. Lemma S7). The upper bound in Eq. (12) follows from Eq. (9) in the main text. Note that this is the best linear upper bound for $\gamma_2^F(F, \mu)$.

To prove Eq. (13) in Theorem 3, note that

$$\begin{aligned} \gamma^F(F, \mu) &= \max_{\rho} \{\gamma(\rho, \mu) | F_B(\rho) \leq F, \rho^2 = \rho\} \\ &\leq \begin{cases} 2F \gamma_2^F(1/2, \mu) & 0 \leq F \leq 1/2, \\ \gamma_2^F(F, \mu) & 1/2 \leq F \leq 1, \end{cases} \end{aligned} \quad (\text{S74})$$

where the inequality follows from Lemma S11 and the monotonicity of $\gamma_2^F(F, \mu)$ in F as shown in Lemma S8.

When $1/2 \leq F \leq 1$, we have $\gamma^F(F, \mu) \geq \gamma_2^F(F, \mu)$ by definition, so Eq. (S74) implies that

$$\begin{aligned} \gamma^F(F, \mu) &= \gamma_2^F(F, \mu) = \gamma_2(2F - 1, \mu) \\ &= \frac{1}{2} + \frac{1}{2} \max_{\mathbf{v}} \int d\mu(\mathbf{r}) \sqrt{(2F - 1)^2 + 4F(1 - F)(\mathbf{r} \cdot \mathbf{v})^2}, \end{aligned} \quad (\text{S75})$$

which confirms Eq. (13). Here the second equality follows from Eq. (12) in Theorem 3 and the third equality follows from Theorem 1.

When $0 \leq F \leq 1/2$, let $\rho' = |\Psi'\rangle\langle\Psi'|$ be a pure product state that satisfies $P_A\rho' = \rho'$, $F_B(\rho') = 1/2$, and $\gamma(\rho', \mu) = \gamma_2^F(1/2, \mu)$. Let $\rho = |\Psi\rangle\langle\Psi|$ with

$$|\Psi\rangle = \sqrt{2F}|\Psi'\rangle + \sqrt{1 - 2F}|22\rangle; \quad (\text{S76})$$

then we have

$$F_B(\rho) = 2FF_B(\rho') = F, \quad (\text{S77})$$

$$\gamma(\rho, \mu) = 2F\gamma(\rho', \mu) = 2F\gamma_2^F(1/2, \mu), \quad (\text{S78})$$

which imply that $\gamma^F(F, \mu) \geq 2F\gamma_2^F(1/2, \mu)$. In conjunction with Eq. (S74), we conclude that

$$\begin{aligned} \gamma^F(F, \mu) &= 2F\gamma_2^F(1/2, \mu) = 2F\gamma_2(0, \mu) = 2\gamma_2^*(\mu)F \\ &= 2\gamma^*(\mu)F. \end{aligned} \quad (\text{S79})$$

Here the second equality follows from Eq. (12) in Theorem 3; the third equality follows from the definition in Eq. (8) in the main text, and the last equality follows from Lemma 1. By virtue of Theorem 1 and Eqs. (7) and (8) in the main text, we can also derive a more explicit expression for $\gamma^F(F, \mu)$,

$$\gamma^F(F, \mu) = F + Fg^*(\mu) = F + F \max_{\mathbf{v}} \int d\mu(\mathbf{r}) |\mathbf{r} \cdot \mathbf{v}|. \quad (\text{S80})$$

Finally, we can prove Eq. (14) in Theorem 3. When $1/2 \leq F \leq 1$, Eq. (14) follows from Eqs. (12) and (13) in Theorem 3, and it offers the best linear upper bound for the guessing probability $\gamma^F(F, \mu)$. When $0 \leq F \leq 1/2$, Eq. (14) follows from Eq. (13) and the simple inequality $\gamma^*(\mu) \geq 1/2$, which is clear from Eq. (8) in the main text. This observation completes the proof of Theorem 3. \square

SUPPLEMENTARY NOTE 6: SAMPLE EFFICIENCY OF SDI QSV

In this section we clarify the sample efficiency of SDI QSV over an untrusted quantum network, in which some parties, but not all, are honest. For simplicity, let us first consider the verification of the two-qubit Bell state $|\Phi\rangle = (|00\rangle + |11\rangle)/\sqrt{2}$. To quantify the closeness between

the actual state ρ and the target state $|\Phi\rangle$, here we adopt the reduced fidelity

$$F_B(\rho) = \max_{U_B} \langle \Phi | (\mathbb{I}_A \otimes U_B) \rho (\mathbb{I}_A \otimes U_B)^\dagger | \Phi \rangle, \quad (\text{S81})$$

as defined in Eq. (11) in the main text, where the maximization is taken over all local unitary transformations on \mathcal{H}_B .

A key to determining the sample efficiency is the relation between the guessing probability and the reduced fidelity as presented in Theorem 3 in the main text. The linear upper bound for $\gamma^F(F, \mu)$ in Eq. (14) is particularly important and is reproduced below,

$$\gamma^F(F, \mu) \leq 1 - 2(1 - \gamma^*)(1 - F). \quad (\text{S82})$$

Given a verification protocol specified by the distribution μ and any state ρ with $F_B(\rho) \leq 1 - \epsilon$, then the probability that ρ can pass one test satisfies

$$p \leq 1 - 2(1 - \gamma^*)\epsilon. \quad (\text{S83})$$

Now suppose the states $\rho_1, \rho_2, \dots, \rho_N$ prepared in N runs are independent of each other. Let $\epsilon_j = 1 - F_B(\rho_j)$; then the probability that these states can pass all N tests satisfies the following inequalities,

$$\prod_{j=1}^N p_j \leq \prod_{j=1}^N [1 - 2(1 - \gamma^*)\epsilon_j] \leq [1 - 2(1 - \gamma^*)\bar{\epsilon}]^N, \quad (\text{S84})$$

where $\bar{\epsilon} = \sum_j \epsilon_j / N$ is the average infidelity. In order to ensure the condition $\bar{\epsilon} < \epsilon$ with significance level δ (confidence level $1 - \delta$), that is, to ensure the condition $\prod_j p_j \leq \delta$ when $\bar{\epsilon} \geq \epsilon$, it suffices to perform

$$N = \left\lceil \frac{\ln \delta}{\ln[1 - 2(1 - \gamma^*)\epsilon]} \right\rceil \approx \frac{\ln \delta^{-1}}{2(1 - \gamma^*)\epsilon} \quad (\text{S85})$$

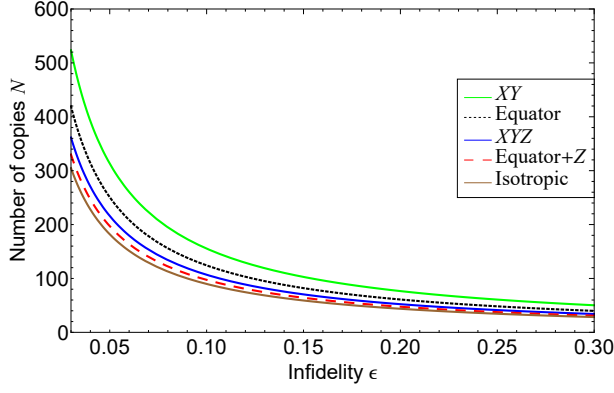
tests, which scale as $N = O(1/(1 - \gamma^*)\epsilon)$. This equation demonstrates the importance of the threshold γ^* in determining the verification efficiency. A small threshold γ^* means a high efficiency.

The minimum threshold $\gamma^* = 3/4$ is achieved for the isotropic protocol (cf. Supplementary Note 9 or Table I in the main text), in which case we have

$$N \approx \frac{2 \ln \delta^{-1}}{\epsilon}. \quad (\text{S86})$$

Surprisingly, this number is comparable to the number $(3 \ln \delta^{-1})/(2\epsilon)$ required in standard QSV [5, 12]. Therefore, SDI verification of the Bell state is almost as efficient as standard QSV. The sample efficiencies of the isotropic protocol and several other protocols in the SDI scenario are illustrated in Supplementary Figure 2.

The above results can be generalized to the verification of the GHZ state following a similar analysis as presented in the main text. Now the threshold is minimized at an equator+ Z protocol with $\gamma^* \approx 0.769$ (cf. Table I).



Supplementary Figure 2. Number of copies needed to verify the Bell state in the SDI scenario for various verification protocols. Here the XY protocol and isotropic protocol are introduced in the main text, while other protocols are proposed in Supplementary Note 9. The significance level is chosen to be $\delta = 0.01$.

Accordingly, the number of tests required to achieve infidelity ϵ and significance level δ reads

$$N \approx \frac{2.16 \ln \delta^{-1}}{\epsilon}. \quad (\text{S87})$$

As in the verification of the Bell state, this number is comparable to the number $(3 \ln \delta^{-1})/(2\epsilon)$ required in standard QSV [13].

To understand the efficiency of our verification protocols proposed for the the SDI scenario, note that each protocol is tied to a steering inequality whose quantum bound and algebraic bound are both equal to 1. This bound corresponds to the maximal probability of passing each test on average and can be attained by a quantum strategy. In addition, the guessing probability threshold is the maximal guessing probability that can be achieved by a classical strategy. As we shall see in Supplementary Note 7, such a high efficiency cannot be achieved in the DI scenario in general unless there exists a suitable Bell inequality for which the quantum bound coincides with the algebraic bound.

Comparison with Refs. [1, 2]

Here we compare our results with previous results in Refs. [1, 2], which studied the self-testing of the Bell state in the one-sided DI scenario, which corresponds to the SDI scenario considered in this work. Both works focused on the steering inequality [1, 2]

$$S = \langle \psi | Z \otimes Z' | \psi \rangle + \langle \psi | X \otimes X' | \psi \rangle \leq \sqrt{2}, \quad (\text{S88})$$

where Z, X are trusted Pauli measurements on Alice's side and Z', X' are untrusted measurements on Bob's side. Both quantum bound and algebraic bound of this inequality are $S_Q = 2$, which can be achieved by the

quantum strategy with ideal measurements on the Bell state $|\Phi\rangle = (|00\rangle + |11\rangle)/\sqrt{2}$. Verification protocol based on this steering inequality is essentially equivalent to the XY protocol considered in this work, which can be regarded as a steering inequality with quantum bound 1 and classical bound $\gamma^* = \frac{1}{2} + \frac{1}{2\sqrt{2}}$.

Both works Refs. [1, 2] provided robust self-testing statements in the one-sided DI scenario. For the steering correlation $S \geq 2 - \epsilon$, Ref. [1] obtained an analytic bound of $13\sqrt{\epsilon}$ and a numeric bound of $\sqrt{\epsilon}$ on the trace distance with the target state, while Ref. [2] obtained an analytic bound of $(3\sqrt{2}+8)\sqrt{\epsilon} + \epsilon/2$. For comparison, here we analyze the performance of the XY protocol with respect to the trace distance. Since the guessing probability in the XY protocol can be rewritten as $\gamma = \frac{1}{2} + \frac{S}{2S_Q}$, combining Eq. (S82), the reduced infidelity can be bounded from above as $1 - F \leq \epsilon/[2(2 - \sqrt{2})]$, so the trace distance can be upper bounded by $\sqrt{\epsilon}/\sqrt{2(2 - \sqrt{2})} \approx 0.924\sqrt{\epsilon}$, which is tighter than previous results.

Ref. [1] also studied the verification of the tripartite GHZ state in both 1-trusted setting and 2-trusted setting, which correspond to different types of multipartite EPR-steering. Numerical results are obtained for both settings based on steering inequalities derived from the Mermin inequality. The scenario considered in this work is more similar to the 2-trusted setting since we assume that each party can only perform local projective measurements. Our result shows that the robustness in the SDI scenario is higher than that in the DI scenario, which is consistent with the result in Ref. [1].

Comparison with Refs. [23, 24]

Next we compare our results with previous results in Refs. [3, 4], which studied the verification of GHZ states in the SDI scenario as considered in this work. The XY protocol considered in this work is equivalent to the protocol proposed in Ref. [3], and the equator protocol is equivalent to the θ -protocol proposed in Ref. [4]. The authors of Refs. [3, 4] derived the guessing probability thresholds $\gamma^* = \frac{1}{2} + \frac{1}{2\sqrt{2}} \approx 0.854$ for the XY protocol and $\gamma^* = \frac{1}{2} + \frac{1}{\pi} \approx 0.818$ for the θ -protocol. In addition, they derived the relation

$$p \leq 1 - \frac{\epsilon}{4} \quad (\text{S89})$$

between the guessing probability and the reduced infidelity for both protocols. However, this relation is suboptimal compared with our result in Eq. (S83), which offers the best linear upper bound for the guessing probability. In addition, Refs. [3, 4] did not consider the sample efficiency. If Eq. (S89) were combined with our analysis above, then the number of tests required to achieve infidelity ϵ and significance level δ would be $N \approx 4(\ln \delta^{-1})/\epsilon$. For comparison, by virtue of Eqs. (S83) and (S85), we

can derive $N \approx 3.41(\ln \delta^{-1})/\epsilon$ for the XY protocol and $N \approx 2.75(\ln \delta^{-1})/\epsilon$ for the equator protocol.

In addition to the efficiency advantage mentioned above, the main merit of our work is to propose a simple approach for determining all potential tests of the GHZ state that are based on local projective measurements. In particular, we prove that only two types of tests can be constructed from local projective measurements (cf. Supplementary Note 10). By virtue of this result, we determine the optimal protocol for verifying the GHZ state and for certifying GME. Such optimality results are difficult to establish and are thus quite rare in the DI and SDI scenarios. Meanwhile, our XYZ protocol, which requires only three measurement settings, is more efficient than all protocols known in the literature even based on infinite measurement settings. The protocols in Refs. [3, 4] are suboptimal because they employ only the second type of tests and their theoretical analyses are suboptimal.

SUPPLEMENTARY NOTE 7: COMPARISON WITH STANDARD QSV AND DEVICE-INDEPENDENT QSV

To put our work in perspective, in this section we compare SDI QSV with standard QSV [5–7] and DI QSV [8] based on self-testing [9, 10]. To start with, it is instructive to clarify the assumptions underlying these frameworks. In standard QSV, all parties that implement the verification protocol are trustworthy, although the source of the quantum system is not necessarily trustworthy. In DI QSV, the source is not trustworthy and is usually treated as a black-box; meanwhile, all the parties that implement the verification protocol (or the underlying measurement devices) are not trustworthy. In this regard, SDI QSV lies between standard QSV and DI QSV in that some parties are honest, but some others may be dishonest. In a word, the assumptions are strongest in standard QSV and weakest in DI QSV. Accordingly, it is easier to realize standard QSV in experiments than SDI QSV, which in turn is easier than DI QSV.

The verification problems in the three scenarios can all be summarized as follows. A quantum device is supposed to produce the target state $|\Psi\rangle \in \mathcal{H}$, but actually produces the states $\rho_1, \rho_2, \dots, \rho_N$ in N runs. For simplicity we assume that the states prepared in different runs are independent of each other. Our task is to verify whether these states are sufficiently close to the target state on average. It should be pointed out that the quantification of closeness depends on the specific scenario under consideration.

Standard quantum state verification

In standard QSV [5–7], all parties implementing the verification protocol are trustworthy; in other words, the measurement devices are trustworthy. A verification pro-

cedure for a given target state $|\Psi\rangle$ is composed of a number of binary tests represented by two-outcome measurements $\{E_l, \mathbb{I} - E_l\}$. Here the test operator E_l corresponds to passing the test and satisfies the condition $E_l|\Psi\rangle = |\Psi\rangle$, so that the target state $|\Psi\rangle$ can always pass the test. Suppose the test $\{E_l, \mathbb{I} - E_l\}$ is performed with probability p_l ; then the verification operator is given by $\Omega = \sum_l p_l E_l$. If $\langle \Psi | \rho_j | \Psi \rangle \leq 1 - \epsilon$, then the average probability that ρ_j can pass each test satisfies [5, 6]

$$\text{tr}(\Omega \rho_j) \leq 1 - [1 - \beta(\Omega)]\epsilon = 1 - \nu(\Omega)\epsilon, \quad (\text{S90})$$

where $\beta(\Omega)$ denotes the second largest eigenvalue of Ω , and $\nu(\Omega) := 1 - \beta(\Omega)$ is the spectral gap from the maximum eigenvalue.

To guarantee that the average infidelity satisfies $\bar{\epsilon} < \epsilon$ with significance level δ , it suffices to perform [5, 6]

$$N = \left\lceil \frac{\ln \delta}{\ln[1 - \nu(\Omega)\epsilon]} \right\rceil \approx \frac{\ln \delta^{-1}}{\nu(\Omega)\epsilon} \quad (\text{S91})$$

tests, which scale as $N = O(1/\nu(\Omega)\epsilon)$. To minimize the number of tests, we need to maximize the value of the spectral gap $\nu(\Omega)$ over all protocols based on LOCC, which is usually extremely difficult if not impossible. So far sample-optimal protocols have been found only for limited classes of states. Fortunately, this problem has been resolved for the Bell state [5, 11, 12] and GHZ states recently [13]. In both cases, the maximum spectral gaps read $\nu(\Omega) = 2/3$, and the numbers of required tests are given by

$$N \approx \frac{3 \ln \delta^{-1}}{2\epsilon}. \quad (\text{S92})$$

Device-independent quantum state verification

Device-independent QSV [8] can be viewed as a verification procedure in the black-box scenario in which measurement devices cannot be trusted. A key for constructing DI verification protocols is self-testing [9, 10], by which quantum states can be certified up to local isometries using only the nonlocal statistics. For example, the maximum quantum bound $2\sqrt{2}$ of the Clauser-Horne-Shimony-Holt (CHSH) inequality [14] certifies the singlet [15]. The maximum quantum bound 4 of the Mermin inequality [16] certifies the tripartite GHZ state [17]. Robustness is the main focus of most studies on self-testing when the correlations achieved deviate from the ideal ones.

On the other hand, to construct a practical DI verification protocol, a self-testing protocol is not enough by itself, unless practical issues like sample efficiency and confidence level can be clarified. Unfortunately, the sample complexity of DI QSV has received little attention until the recent work of Dimić et al. [8] although there are numerous works on self-testing (see Ref. [10] for a review). Following Refs. [8, 17], here we discuss the sample efficiency of DI verification of the tripartite GHZ state

based on self-testing results tied to the Mermin inequality.

In self-testing, the *extractability* [17] is used to quantify the closeness between the actual state ρ and the target state $|\Psi\rangle$; it is defined as

$$\Theta(\rho, |\Psi\rangle) := \max_{\Lambda} F(\Lambda(\rho), |\Psi\rangle), \quad (\text{S93})$$

where the maximization is taken over all local isometries. Suppose the Bell inequality \mathcal{B} is used to self-test the target state $|\Psi\rangle$. Denote by β_C and β_Q the maximal classical bound and quantum bound of \mathcal{B} , respectively. To determine the sample complexity, we need to clarify the relation between the extractability and the Bell violation. The extractability-violation trade-off is characterized by the function $\mathcal{Q}_{\Psi, \mathcal{B}} : [\beta_C, \beta_Q] \rightarrow [0, 1]$ defined as [17]:

$$\mathcal{Q}_{\Psi, \mathcal{B}}(\beta) := \inf_{\rho_{AB} \in \mathcal{S}_{\mathcal{B}}(\beta)} \Theta(\rho_{AB}, \Psi), \quad (\text{S94})$$

where $\mathcal{S}_{\mathcal{B}}(\beta)$ denotes the set of quantum states that can achieve the violation β for the Bell inequality \mathcal{B} . This function sets a lower bound on the extractability given the observed violation β .

To be concrete, let us consider self-testing of the tripartite GHZ state using the Mermin inequality. Recall that the Mermin operator reads

$$\mathcal{B}_{\text{Mermin}} = \sum_{j,k \in \{0,1\}} (-1)^{jk} A_j \otimes B_k \otimes C_{j \oplus k}, \quad (\text{S95})$$

where A_j are binary observables (with eigenvalues ± 1) for Alice (the observables for Bob and Charlie have the same structure). The quantum bound of the Mermin inequality is $\beta_Q = 4$, which coincides with the algebraic bound. The extractability-violation function was determined in Ref. [17], with the result

$$\mathcal{Q}_{G^3, \mathcal{B}_{\text{Mermin}}}(\beta) \geq \frac{1}{2} + \frac{1}{2} \cdot \frac{\beta - \beta^*}{\beta_Q - \beta^*}, \quad (\text{S96})$$

where $\beta_Q = 4$ is the quantum bound and $\beta^* = 2\sqrt{2}$ is the threshold violation [17]. Notably, for any state ρ with $\Theta(\rho, \Psi) \leq 1 - \epsilon$, the Bell violation β it can achieve satisfies

$$\frac{1}{2} + \frac{1}{2} \cdot \frac{\beta - \beta^*}{\beta_Q - \beta^*} \leq 1 - \epsilon. \quad (\text{S97})$$

Since the quantum bound coincides with the algebraic bound for the Mermin inequality, the self-testing procedure determined by Eq. (S95) can be turned into a DI verification protocol with four tests chosen with probability $1/4$ each. Note that the target GHZ state can always pass each test. It remains to establish the relation between the guessing probability and the extractability. For a generic state ρ , the average probability of passing each test reads $p = \frac{1}{2} + \frac{\beta}{2\beta_Q}$, where β is the Bell violation. If $\Theta(\rho, \Psi) \leq 1 - \epsilon$, then Eq. (S97) implies that

$$p \leq 1 - \left(1 - \frac{\beta^*}{\beta_Q}\right) \epsilon = 1 - \frac{2 - \sqrt{2}}{2} \epsilon. \quad (\text{S98})$$

Now we are ready to estimate the number of copies needed to achieve a given extractability in DI verification of the tripartite GHZ state. Suppose the states $\rho_1, \rho_2, \dots, \rho_N$ prepared in N runs are independent of each other. Then the probability that these states can pass all N tests is upper bounded by

$$\left(1 - \frac{2 - \sqrt{2}}{2} \bar{\epsilon}\right)^N, \quad (\text{S99})$$

where $1 - \bar{\epsilon}$ denotes the average extractability. In order to insure the condition $\bar{\epsilon} < \epsilon$ with significance level δ , it suffices to perform

$$N = \left\lceil \frac{\ln \delta}{\ln \left[1 - \frac{2 - \sqrt{2}}{2} \epsilon\right]} \right\rceil \approx \frac{2 \ln \delta^{-1}}{(2 - \sqrt{2}) \epsilon} \approx \frac{3.41 \ln \delta^{-1}}{\epsilon} \quad (\text{S100})$$

tests. Surprisingly, the scaling behaviors of N in ϵ and δ for DI QSV are the same as the counterparts for standard QSV and SDI QSV considered in this work; moreover, the constant coefficients for the three scenarios are quite close to each other.

It should be pointed out that the above analysis is applicable only when the quantum bound of the underlying Bell inequality coincides with the algebraic bound. If this condition does not hold, then the situation gets more complicated [8], and the optimal scaling behaviors shown in Eq. (S100) cannot be guaranteed. Now the number of tests required reads

$$N = O\left(\frac{\ln \delta^{-1}}{c^2 \epsilon^2}\right), \quad (\text{S101})$$

where c is a constant characterizing the linear dependence between the extractability and the Bell violation. For example, Eq. (S101) holds in DI verification of the Bell state based on the CHSH inequality. Here the sample efficiency is suboptimal compared with the counterparts in standard QSV and SDI QSV (cf. Supplementary Note 6).

SUPPLEMENTARY NOTE 8: VERIFICATION PROTOCOLS BASED ON DISCRETE DISTRIBUTIONS

Recall that each verification protocol of the Bell state is specified by a probability distribution on the Bloch sphere. In practice, it is usually more convenient to choose a discrete distribution as specified by a weighted set $\{\mathbf{r}_j, p_j\}_j$, where $S = \{\mathbf{r}_j\}_j$ is a set of unit vectors on the Bloch sphere, and $\{p_j\}_j$ is a probability distribution. This weighted set means the projective measurement \mathbf{r}_j is performed with probability p_j . When all the probabilities p_j are equal, the weighted set $\{\mathbf{r}_j, p_j\}_j$ is abbreviated as $S = \{\mathbf{r}_j\}_j$ to simplify the notation. All results presented in the main text and in this Supplementary Material hold for discrete distributions as well

as for continuous distributions. For example, Theorem 1 implies that

$$g(C, \{\mathbf{r}_j, p_j\}_j) = \max_{\mathbf{v}} \sum_j p_j \sqrt{C^2 + (1 - C^2)(\mathbf{r}_j \cdot \mathbf{v})^2}. \quad (\text{S102})$$

When $C = 0$, Eq. (S102) reduces to

$$g^*(\{\mathbf{r}_j, p_j\}_j) = \max_{\mathbf{v}} \sum_j p_j |\mathbf{r}_j \cdot \mathbf{v}|. \quad (\text{S103})$$

Incidentally, the verification matrix defined in Eq. (S11) now reduces to

$$\Xi(\mu) = \Xi(\{\mathbf{r}_j, p_j\}_j) = \sum_j p_j \mathbf{r}_j \mathbf{r}_j^T. \quad (\text{S104})$$

When all p_j are equal, Eq. (S103) further reduces to

$$g^*(S) = \frac{1}{|S|} \max_{\mathbf{v}} \sum_{\mathbf{r} \in S} |\mathbf{r} \cdot \mathbf{v}|, \quad (\text{S105})$$

where $|S|$ denotes the cardinality of S .

Lemma S12. *Suppose the symmetry group of $\{\mathbf{r}_j\}_j$ acts transitively. Then $g(C, \{\mathbf{r}_j, p_j\}_j)$ for a given set $\{\mathbf{r}_j\}_j$ is minimized when all p_j are equal.*

Lemma S12 follows from Lemma S1. It applies in particular when $\{\mathbf{r}_j\}_j$ forms a platonic solid or a regular polygon.

Let S be a set of unit vectors on the Bloch sphere and let \mathbf{v} be a unit vector on the Bloch sphere. The set S is center symmetric if $\mathbf{r} \in S$ means $-\mathbf{r} \in S$ and vice versa. Define

$$\boldsymbol{\eta}(S) := \sum_{\mathbf{r} \in S} \mathbf{r}, \quad (\text{S106})$$

$$S_{\mathbf{v}} := \{\mathbf{r} \in S \mid \mathbf{r} \cdot \mathbf{v} \geq 0\}. \quad (\text{S107})$$

Lemma S13. *Let $S = \{\mathbf{r}_j\}_{j=1}^M$ be a set of M unit vectors on the Bloch sphere that is center symmetric. Then*

$$g^*(S) = \frac{1}{M} \max_{\mathbf{v}} \sum_{j=1}^M |\mathbf{r}_j \cdot \mathbf{v}| \quad (\text{S108})$$

$$= \frac{2}{M} \max_{\mathbf{v}} |\boldsymbol{\eta}(S_{\mathbf{v}})| \quad (\text{S109})$$

$$= \frac{2}{M} \max_{S' \subseteq S} |\boldsymbol{\eta}(S')|. \quad (\text{S110})$$

If the maximum in Eq. (S110) is attained at the set S' , then S' contains exactly $M/2$ vectors; in addition,

$$\boldsymbol{\eta}(S') \cdot \mathbf{r} \geq \frac{1}{2} \quad \forall \mathbf{r} \in S', \quad \boldsymbol{\eta}(S') \cdot \mathbf{r} \leq -\frac{1}{2} \quad \forall \mathbf{r} \in \overline{S'}, \quad (\text{S111})$$

where $\overline{S'}$ is the complement of S' in S . If the maximum in Eq. (S108) is attained at the unit vector \mathbf{v} , so that \mathbf{v} is an intelligent direction at $C = 0$, then

$$\mathbf{v} \parallel \boldsymbol{\eta}(S_{\mathbf{v}}), \quad \mathbf{v} \cdot \mathbf{r}_j \neq 0 \quad \forall j. \quad (\text{S112})$$

Lemma S13 also implies that an optimal set S' that maximizes $|\boldsymbol{\eta}(S')|$ contains exactly one vector in the set $\{\mathbf{r}, -\mathbf{r}\}$ for each $\mathbf{r} \in S$.

Proof. Equations (S108)-(S110) follow from Eq. (S105) and Lemma S6; note that the condition in Eq. (S26) is guaranteed by the assumption that $\{\mathbf{r}_j\}_{j=1}^M$ is center symmetric.

Suppose the maximum in Eq. (S110) is attained at the set S' . Then

$$|\boldsymbol{\eta}(S') - \mathbf{r}|^2 \leq |\boldsymbol{\eta}(S')|^2 \quad \forall \mathbf{r} \in S', \quad (\text{S113})$$

$$|\boldsymbol{\eta}(S') + \mathbf{r}|^2 \leq |\boldsymbol{\eta}(S')|^2 \quad \forall \mathbf{r} \in \overline{S'}, \quad (\text{S114})$$

which imply Eq. (S111). As a corollary, S' contains exactly one vector in the set $\{\mathbf{r}, -\mathbf{r}\}$ for each $\mathbf{r} \in S$. In particular, S' has cardinality $M/2$.

Next, suppose the maximum in Eq. (S108) is attained at the unit vector \mathbf{v} . Then $\mathbf{v} \parallel \boldsymbol{\eta}(S_{\mathbf{v}})$ by Lemma S6, and the maximum in Eq. (S110) is attained at the set $S_{\mathbf{v}}$. In addition, $\boldsymbol{\eta}(S_{\mathbf{v}}) \cdot \mathbf{r}_j \neq 0$ for all j according to Eq. (S111), so $\mathbf{v} \cdot \mathbf{r}_j \neq 0$ for all j . \square

SUPPLEMENTARY NOTE 9: CONCRETE VERIFICATION PROTOCOLS

Here we study various concrete protocols for verifying the Bell state in the presence of a dishonest party. In addition to the verification protocols listed in Table I, we also consider protocols based on platonic solids and arbitrary regular polygons (with extension by including the Z measurement). Given a verification protocol specified by a distribution μ on the Bloch sphere, our main goal is to determine $g(C, \mu)$, $\gamma(C, \mu) = \gamma_2(C, \mu)$, $\gamma^*(\mu) = \gamma_2^*(\mu) = \gamma_2(0, \mu)$, and $\hat{\gamma}(C, \mu) = \hat{\gamma}_2(C, \mu)$ (cf. Theorems 1, 2, and Lemma 1 in the main text). Furthermore, we determine the optimal protocol and the optimal two-setting protocol. The main results are summarized in Table I in the main text. Many protocols presented here can easily be adapted for the verification of GHZ states.

Two-setting protocols

In the simplest verification protocol, Alice can perform two projective measurements \mathbf{r}_1 and \mathbf{r}_2 with probabilities p_1 and p_2 , respectively. By replacing \mathbf{r}_2 with $-\mathbf{r}_2$ if necessary, we can assume that $\mathbf{r}_1 \cdot \mathbf{r}_2 \geq 0$. To minimize the guessing probability of Bob, Alice can choose $p_1 = p_2 = 1/2$ according to Lemma S12; then the verification matrix reads

$$\Xi = \frac{1}{2}(\mathbf{r}_1 \mathbf{r}_1^T + \mathbf{r}_2 \mathbf{r}_2^T). \quad (\text{S115})$$

Let $\alpha = \arccos(\mathbf{r}_1 \cdot \mathbf{r}_2)$; then $0 \leq \alpha \leq \pi/2$ and

$$\|\Xi\| = \frac{1 + \cos \alpha}{2}. \quad (\text{S116})$$

In addition, Lemma S2 implies that

$$\begin{aligned} g(C, \mu) &= \sqrt{\frac{1 + \cos \alpha + C^2(1 - \cos \alpha)}{2}} \\ &= \sqrt{\frac{1 + C^2 + (1 - C^2) \cos \alpha}{2}}; \end{aligned} \quad (\text{S117})$$

meanwhile, any unit vector parallel to $\mathbf{r}_1 + \mathbf{r}_2$ represents an intelligent direction. Here $g(C, \mu)$ is minimized when $\alpha = \pi/2$, so that \mathbf{r}_1 and \mathbf{r}_2 are orthogonal, in which case we obtain the optimal two-setting protocol with

$$g(C, \mu) = \sqrt{\frac{1 + C^2}{2}}, \quad \gamma_2(C, \mu) = \frac{1}{2} + \frac{1}{2} \sqrt{\frac{1 + C^2}{2}}. \quad (\text{S118})$$

The special case XY protocol was proposed previously in Ref. [3]. However, Ref. [3] neither derived the exact formula for the guessing probability nor proved the optimality of the XY protocol among all two-setting protocols.

When $C = 0$, Eq. (S118) yields

$$g^*(\mu) = \frac{1}{\sqrt{2}}, \quad \gamma_2^*(\mu) = \frac{1}{2} + \frac{1}{2\sqrt{2}}. \quad (\text{S119})$$

By virtue of Theorem 2 we can further deduce that

$$\hat{\gamma}_2(C, \mu) = \frac{1 + C}{2} + \frac{1 - C}{2\sqrt{2}} = \frac{1}{4}[2 + \sqrt{2} + (2 - \sqrt{2})C]. \quad (\text{S120})$$

Proposition 1. Suppose μ is a two-setting protocol specified by the weighted set $\{\mathbf{r}_j, p_j\}_{j=1}^2$. Then

$$g(C, \mu) \geq \sqrt{\frac{1 + C^2}{2}}, \quad \gamma_2(C, \mu) \geq \frac{1}{2} + \frac{1}{2} \sqrt{\frac{1 + C^2}{2}}, \quad (\text{S121})$$

$$\hat{\gamma}_2(C, \mu) \geq \frac{1}{4}[2 + \sqrt{2} + (2 - \sqrt{2})C]. \quad (\text{S122})$$

When $0 \leq C < 1$, the three inequalities are saturated iff $\mathbf{r}_1, \mathbf{r}_2$ are orthogonal and $p_1 = p_2 = 1/2$.

Proof. According to the above discussion, the three inequalities in Eqs. (S121) and (S122) hold for all two-setting protocols. In addition they are saturated if $\mathbf{r}_1, \mathbf{r}_2$ are orthogonal and $p_1 = p_2 = 1/2$. When $0 \leq C < 1$, if one of the inequalities is saturated, then the other two are also saturated thanks to Eq. (5) and Theorem 2 in the main text, so we have $g(C, \mu) = \sqrt{(1 + C^2)/2}$. According to Eq. (S117) and the above discussion, $\mathbf{r}_1, \mathbf{r}_2$ must be orthogonal. By Eq. (S102) we have

$$\begin{aligned} g(C, \mu) &= \max_{x^2 + y^2 \leq 1} \left(p_1 \sqrt{C^2 + (1 - C^2)x^2} \right. \\ &\quad \left. + p_2 \sqrt{C^2 + (1 - C^2)y^2} \right) \\ &\geq \max_{x^2 + y^2 \leq 1} \sqrt{C^2 + (1 - C^2)(p_1 x + p_2 y)^2} \\ &= \sqrt{C^2 + (1 - C^2)(p_1^2 + p_2^2)} \geq \sqrt{\frac{1 + C^2}{2}}, \end{aligned} \quad (\text{S123})$$

where the first inequality follows from the fact that $\sqrt{C^2 + (1 - C^2)x^2}$ is convex in x . The last inequality is saturated iff $p_1 = p_2 = 1/2$. This observation completes the proof of Proposition 1. \square

Three-setting protocols

Here we consider verification protocols based on three measurement settings. We are particularly interested in the case in which the Bloch vectors $\mathbf{r}_1, \mathbf{r}_2, \mathbf{r}_3$ that specify the three projective measurements are mutually orthogonal, so that the corresponding projective measurements are mutually unbiased. For example, the measurement bases can be chosen to be the eigenbases of the three Pauli operators X, Y, Z , which lead to the XYZ protocol. To minimize the guessing probability, the three measurements should be performed with the equal probability of $1/3$ according to Lemma S12. In this case, the verification matrix reads $\Xi(\mu) = \mathbb{I}/3$, and the bound in Lemma S2 can be saturated, so we have

$$g(C, XYZ) = \sqrt{\frac{1 + 2C^2}{3}}, \quad (\text{S124})$$

$$\gamma_2(C, XYZ) = \frac{1}{2} + \frac{1}{2} \sqrt{\frac{1 + 2C^2}{3}}. \quad (\text{S125})$$

When $0 \leq C < 1$, there are eight intelligent directions, namely, $(\pm 1, \pm 1, \pm 1)^T / \sqrt{3}$. When $C = 0$, the above two equations reduce to

$$g^*(XYZ) = \frac{1}{\sqrt{3}}, \quad \gamma_2^*(XYZ) = \frac{1}{2} + \frac{1}{2\sqrt{3}}. \quad (\text{S126})$$

By virtue of Theorem 2 we can further deduce that

$$\hat{\gamma}_2(C, XYZ) = \frac{1}{6}[3 + \sqrt{3} + (3 - \sqrt{3})C]. \quad (\text{S127})$$

Thanks to Proposition 2 below, the XYZ protocol is optimal among all three-setting protocols with respect to $\gamma_2^*(\mu)$ and $\hat{\gamma}_2(C, \mu)$.

Proposition 2. Suppose μ is a three-setting protocol specified by the weighted set $\{\mathbf{r}_j, p_j\}_{j=1}^3$. Then

$$g^*(\mu) \geq \frac{1}{\sqrt{3}}, \quad \gamma_2^*(\mu) \geq \frac{3 + \sqrt{3}}{6}, \quad (\text{S128})$$

$$\hat{\gamma}_2(C, \mu) \geq \frac{1}{6}[3 + \sqrt{3} + (3 - \sqrt{3})C]. \quad (\text{S129})$$

The inequalities in Eq. (S128) are saturated iff $\mathbf{r}_1, \mathbf{r}_2, \mathbf{r}_3$ are mutually orthogonal and $p_1 = p_2 = p_3 = 1/3$. When $0 \leq C < 1$, the inequality in Eq. (S129) is saturated iff the same conditions hold.

Proof. The two inequalities in Eq. (S128) are equivalent by Eq. (5) in the main text and they imply Eq. (S129) thanks to Theorem 2. In addition, $\hat{\gamma}_2(C = 1, \mu) = 1$, and the inequality in Eq. (S129) for any $0 \leq C < 1$ implies the

two inequalities in Eq. (S128). So it suffices to consider the first inequality $g^*(\mu) \geq 1/\sqrt{3}$. If one of the three probabilities p_1, p_2, p_3 is equal to 0, then μ reduces to a two-setting protocol, in which case we have

$$g^*(\mu) \geq \frac{1}{\sqrt{2}} > g^*(XYZ) = \frac{1}{\sqrt{3}}. \quad (\text{S130})$$

So the inequalities in Eq. (S128) hold and cannot be saturated.

Next, we consider the case in which $p_1, p_2, p_3 > 0$. Note that the protocol μ is equivalent to the protocol μ' specified by the following weighted set

$$\{\{\mathbf{r}_1, p_1/2\}, \{-\mathbf{r}_1, p_1/2\}, \{\mathbf{r}_2, p_2/2\}, \{-\mathbf{r}_2, p_2/2\}, \{\mathbf{r}_3, p_3/2\}, \{-\mathbf{r}_3, p_3/2\}\}, \quad (\text{S131})$$

which satisfies Eq. (S26) with μ replaced by μ' . According to Lemma S6, we have

$$\begin{aligned} g^*(\mu) &= g^*(\mu') \\ &= \max\{|p_1\mathbf{r}_1 + p_2\mathbf{r}_2 + p_3\mathbf{r}_3|, |p_1\mathbf{r}_1 + p_2\mathbf{r}_2 - p_3\mathbf{r}_3|, \\ &\quad |p_1\mathbf{r}_1 - p_2\mathbf{r}_2 + p_3\mathbf{r}_3|, |p_1\mathbf{r}_1 - p_2\mathbf{r}_2 - p_3\mathbf{r}_3|\} \\ &= \max\left\{\sqrt{(p_1\mathbf{r}_1 + p_2\mathbf{r}_2)^2 + p_3^2 + 2p_3\mathbf{r}_3 \cdot (p_1\mathbf{r}_1 + p_2\mathbf{r}_2)}, \right. \\ &\quad \sqrt{(p_1\mathbf{r}_1 + p_2\mathbf{r}_2)^2 + p_3^2 - 2p_3\mathbf{r}_3 \cdot (p_1\mathbf{r}_1 + p_2\mathbf{r}_2)}, \\ &\quad \sqrt{(p_1\mathbf{r}_1 - p_2\mathbf{r}_2)^2 + p_3^2 + 2p_3\mathbf{r}_3 \cdot (p_1\mathbf{r}_1 - p_2\mathbf{r}_2)}, \\ &\quad \left. \sqrt{(p_1\mathbf{r}_1 - p_2\mathbf{r}_2)^2 + p_3^2 - 2p_3\mathbf{r}_3 \cdot (p_1\mathbf{r}_1 - p_2\mathbf{r}_2)}\right\} \\ &\geq \max\left\{\sqrt{(p_1\mathbf{r}_1 + p_2\mathbf{r}_2)^2 + p_3^2}, \sqrt{(p_1\mathbf{r}_1 - p_2\mathbf{r}_2)^2 + p_3^2}\right\} \\ &= \max\left\{\sqrt{p_1^2 + p_2^2 + p_3^2 + 2p_1p_2(\mathbf{r}_1 \cdot \mathbf{r}_2)}, \right. \\ &\quad \left. \sqrt{p_1^2 + p_2^2 + p_3^2 - 2p_1p_2(\mathbf{r}_1 \cdot \mathbf{r}_2)}\right\} \\ &\geq \sqrt{p_1^2 + p_2^2 + p_3^2} \geq \frac{p_1 + p_2 + p_3}{\sqrt{3}} = \frac{1}{\sqrt{3}}, \end{aligned} \quad (\text{S132})$$

which confirms Eq. (S128). Here the last inequality is saturated iff $p_1 = p_2 = p_3 = 1/3$; the second inequality is saturated iff $\mathbf{r}_1 \perp \mathbf{r}_2$ given that $p_1, p_2, p_3 > 0$. When $\mathbf{r}_1 \perp \mathbf{r}_2$, the first inequality is saturated iff $\mathbf{r}_3 \perp \mathbf{r}_1$ and $\mathbf{r}_3 \perp \mathbf{r}_2$. Therefore, for a three-setting protocol μ , the inequality $g^*(\mu) \geq 1/\sqrt{3}$ is saturated iff $\mathbf{r}_1, \mathbf{r}_2, \mathbf{r}_3$ are mutually orthogonal and $p_1 = p_2 = p_3 = 1/3$. \square

Optimal protocol

Since $g(C, \mu)$ is convex in μ by Lemma S1 and is invariant under rotations on the Bloch sphere, it is minimized when μ is the uniform distribution on the Bloch sphere, which leads to the isotropic protocol. Then the integration in Eq. (6) in the main text is independent of the unit vector \mathbf{v} , so any direction is an intelligent direction. For

simplicity we can choose $\mathbf{v} = (0, 0, 1)^T$, which yields

$$\begin{aligned} g(C, \mu) &= \int d\mu(\mathbf{r}) \sqrt{C^2 + (1 - C^2)(\mathbf{r} \cdot \mathbf{v})^2} \\ &= \frac{1}{4\pi} \int_{\alpha=0}^{\pi} d\alpha \int_{\phi=0}^{2\pi} d\phi \sin \alpha \sqrt{C^2 + (1 - C^2) \cos^2 \alpha} \\ &= \int_0^1 dx \sqrt{C^2 + (1 - C^2)x^2} \\ &= \frac{1}{2} + \frac{C^2 \text{arcsinh}(\frac{\sqrt{1-C^2}}{C})}{2\sqrt{1-C^2}}. \end{aligned} \quad (\text{S133})$$

In the limit $C \rightarrow 0$, this equation yields

$$g^*(\mu) = \frac{1}{2}, \quad \gamma_2^*(\mu) = \frac{3}{4}. \quad (\text{S134})$$

By virtue of Theorem 2 we can further deduce that

$$\hat{\gamma}_2(C, \mu) = \frac{1+C}{2} + \frac{1-C}{4} = \frac{3+C}{4}. \quad (\text{S135})$$

The above discussion yields the following proposition.

Proposition 3. *Every verification protocol μ of the Bell state satisfies*

$$g(C, \mu) \geq \frac{1}{2} + \frac{C^2 \text{arcsinh}(\frac{\sqrt{1-C^2}}{C})}{2\sqrt{1-C^2}}, \quad (\text{S136})$$

$$\gamma_2(C, \mu) \geq \frac{3}{4} + \frac{C^2 \text{arcsinh}(\frac{\sqrt{1-C^2}}{C})}{4\sqrt{1-C^2}}, \quad (\text{S137})$$

$$\hat{\gamma}_2(C, \mu) \geq \frac{3+C}{4}. \quad (\text{S138})$$

All inequalities are saturated for the isotropic protocol.

Equator protocol

When the support of μ is contained in the equator, $g(C, \mu)$ is minimized when μ is the uniform distribution on the equator. The resulting protocol is called the equator protocol, which is equivalent to the θ -protocol proposed in Ref. [4]. In this case, the integration in Eq. (6) in the main text is maximized when \mathbf{v} is any unit vector in the xy -plane. In other words, any direction in the xy -plane is an intelligent direction. To simplify the calculation we can choose $\mathbf{v} = (1, 0, 0)^T$, which yields

$$\begin{aligned} g(C, \mu) &= \int d\mu(\mathbf{r}) \sqrt{C^2 + (1 - C^2)(\mathbf{r} \cdot \mathbf{v})^2} \\ &= \frac{1}{2\pi} \int_0^{2\pi} d\phi \sqrt{C^2 + (1 - C^2) \cos^2 \phi} \\ &= \frac{2}{\pi} \int_0^{\pi/2} d\phi \sqrt{1 - (1 - C^2) \sin^2 \phi} \\ &= \frac{2}{\pi} K(\sqrt{1 - C^2}), \end{aligned} \quad (\text{S139})$$

where $K(\sqrt{1-C^2})$ is a complete elliptic integral of the second kind. In conjunction with Eq. (5) in the main text we get

$$\gamma_2(C, \mu) = \frac{1}{2} + \frac{1}{\pi} K(\sqrt{1-C^2}). \quad (\text{S140})$$

When $C = 0$, we have $K(\sqrt{1-C^2}) = 1$ and

$$g^*(\mu) = \frac{2}{\pi}, \quad \gamma_2^*(\mu) = \frac{1}{2} + \frac{1}{\pi}. \quad (\text{S141})$$

By virtue of Theorem 2 we can deduce that

$$\hat{\gamma}_2(C, \mu) = \frac{1+C}{2} + \frac{1-C}{\pi} = \frac{1}{2\pi} [\pi + 2 + (\pi - 2)C]. \quad (\text{S142})$$

The above discussion yields the following proposition.

Proposition 4. *Suppose μ is supported on the equator of the Bloch sphere. Then*

$$g(C, \mu) \geq \frac{2}{\pi} K(\sqrt{1-C^2}), \quad (\text{S143})$$

$$\gamma_2(C, \mu) \geq \frac{1}{2} + \frac{1}{\pi} K(\sqrt{1-C^2}), \quad (\text{S144})$$

$$\hat{\gamma}_2(C, \mu) \geq \frac{1}{2\pi} [\pi + 2 + (\pi - 2)C]. \quad (\text{S145})$$

All inequalities are saturated for the equator protocol.

Polygon protocols

Here we consider verification protocols defined by regular polygons inscribed on the equator of the Bloch sphere. For simplicity, all measurement settings are chosen with the same probability, which is the optimal choice according to Lemma S12. The resulting protocols are called polygon protocols, which may be regarded as discrete versions of the equator protocol.

Consider a polygon with M vertices, without loss of generality, we can assume that the M unit vectors defining the polygon have the form

$$\mathbf{r}_j = (\cos \theta_j, \sin \theta_j, 0)^T, \quad (\text{S146})$$

where

$$\theta_j = \frac{2(j-1)\pi}{M}, \quad j = 1, 2, \dots, M. \quad (\text{S147})$$

Let $g(C, M) := g(C, \{\mathbf{r}_j\}_{j=1}^M)$ and $g^*(M) := g(0, M)$. Then we have

$$\begin{aligned} g(C, M) &= \frac{1}{M} \max_{\mathbf{v}} \sum_{j=1}^M \sqrt{C^2 + (1-C^2)(\mathbf{r}_j \cdot \mathbf{v})^2} \\ &= \frac{1}{M} \max_{0 \leq \varphi < 2\pi} \sum_{j=0}^{M-1} \sqrt{C^2 + (1-C^2) \cos^2 \left(\frac{2\pi j}{M} - \varphi \right)}, \end{aligned} \quad (\text{S148})$$

where the maximization in the first line is taken over all unit vectors on the Bloch sphere. When M goes to infinity, the polygon protocol approaches the equator protocol.

In general it is not easy to derive an analytical formula for $g(C, \mu)$. Here we focus on the special case $C = 0$, which yields the following proposition.

Proposition 5. *For any integer $M \geq 3$ we have*

$$g^*(M) = \begin{cases} 2 \left[M \sin \left(\frac{\pi}{M} \right) \right]^{-1} & M \text{ even,} \\ \left[M \sin \left(\frac{\pi}{2M} \right) \right]^{-1} & M \text{ odd.} \end{cases} \quad (\text{S149})$$

Proposition 5 above and Eq. (5) in the main text together yield

$$\gamma_2^*(M) = \begin{cases} \frac{1}{2} + \left[M \sin \left(\frac{\pi}{M} \right) \right]^{-1} & M \text{ even,} \\ \frac{1}{2} + \left[2M \sin \left(\frac{\pi}{2M} \right) \right]^{-1} & M \text{ odd.} \end{cases} \quad (\text{S150})$$

By virtue of Theorem 2 we can further deduce that

$$\hat{\gamma}_2(C, M) = \begin{cases} \frac{1+C}{2} + \frac{1-C}{M \sin \left(\frac{\pi}{M} \right)} & M \text{ even,} \\ \frac{1+C}{2} + \frac{1-C}{2M \sin \left(\frac{\pi}{2M} \right)} & M \text{ odd.} \end{cases} \quad (\text{S151})$$

Proof of Proposition 5. When $C = 0$, Eq. (S148) yields

$$\begin{aligned} g^*(M) &= \frac{1}{M} \max_{\mathbf{v}} \sum_{j=1}^M |\mathbf{r}_j \cdot \mathbf{v}| \\ &= \frac{1}{M} \max_{0 \leq \varphi < 2\pi} \sum_{j=0}^{M-1} \left| \cos \left(\frac{2\pi j}{M} - \varphi \right) \right|. \end{aligned} \quad (\text{S152})$$

When M is even, let $S = \{\mathbf{r}_1, \mathbf{r}_2, \dots, \mathbf{r}_{M/2}\}$ be a set of $M/2$ unit vectors, which correspond to $M/2$ consecutive vertices of the polygon. Then Lemma S13 implies that

$$\begin{aligned} g^*(M) &= \frac{2}{M} |\boldsymbol{\eta}(S)| = \frac{2}{M} \left| \sum_{j=1}^{M/2} \mathbf{r}_j \right| = \frac{2}{M} \left| \sum_{j=1}^{M/2} e^{i\theta_j} \right| \\ &= \frac{2}{M} \frac{2}{|1 - e^{2\pi i/M}|} = \frac{2}{M \sin \left(\frac{\pi}{M} \right)}, \end{aligned} \quad (\text{S153})$$

which confirms Eq. (S149). Alternatively, this result can be derived directly by virtue of Eq. (S152).

When M is even but not divisible by 4, Lemma S13 also implies that each intelligent direction coincides with some \mathbf{r}_j . When M is divisible by 4, by contrast, each intelligent direction passes through the middle point of some edge of the polygon.

When M is odd, the polygon protocol with M measurement settings is equivalent to the polygon protocol with $2M$ measurement settings. So each intelligent direction coincides with some \mathbf{r}_j or $-\mathbf{r}_j$, and we have

$$g^*(M) = g^*(2M) = \left[M \sin \left(\frac{\pi}{2M} \right) \right]^{-1}. \quad (\text{S154})$$

This observation completes the proof of Proposition 5. \square

When $C > 0$, numerical calculation indicates that each intelligent direction for $C = 0$ is still an intelligent direction for $C > 0$. To be concrete, when M is not divisible by 4, any unit vector parallel or antiparallel to \mathbf{r}_j is an

intelligent direction. When M is divisible by 4, by contrast, any unit vector passing through the middle point of some edge of the polygon is an intelligent direction. This observation leads to the following conjecture.

Conjecture 1. *Suppose $M \geq 3$ is an integer and $0 \leq C \leq 1$; then we have*

$$g(C, M) = \begin{cases} \frac{1}{M} \sum_{j=0}^{M-1} \sqrt{C^2 + (1 - C^2) \cos^2\left(\frac{(2j-1)\pi}{M}\right)} & 4|M, \\ \frac{1}{M} \sum_{j=0}^{M-1} \sqrt{C^2 + (1 - C^2) \cos^2\left(\frac{2j\pi}{M}\right)} & 4 \nmid M. \end{cases} \quad (\text{S155})$$

When $M = 3$, the maximization over φ in Eq. (S148) can be solved directly by considering the derivative over φ , which yields

$$g(C, 3) = \frac{1 + \sqrt{1 + 3C^2}}{3}, \quad \gamma_2(C, 3) = \frac{4 + \sqrt{1 + 3C^2}}{6} \quad (\text{S156})$$

and confirms Conjecture 1. When $C = 0$, this equation reduces to

$$g^*(3) = \frac{2}{3}, \quad \gamma_2^*(3) = \frac{5}{6}, \quad (\text{S157})$$

which agrees with Proposition 5.

In the limit $M \rightarrow \infty$, the polygon protocol approaches the equator protocol; accordingly, the above results converge to the counterparts for the equator protocol.

Equator+Z protocol

Equator+Z protocol is another protocol of special interest, especially in the verification of GHZ states. The corresponding distribution μ is concentrated on the equator together with the north and south poles. To minimize $g(C, \mu)$, the distribution μ should be uniform on the equator. Let p be the total probability assigned to the north and south poles. Thanks to the rotation symmetry around the z -axis, Eq. (6) can be simplified as follows,

$$g(C, \mu) = \max_{0 \leq \alpha \leq \pi/2} \left[p \sqrt{C^2 + (1 - C^2) \cos^2 \alpha} + \frac{1-p}{2\pi} \int_0^{2\pi} d\phi \sqrt{C^2 + (1 - C^2) \sin^2 \alpha \cos^2 \phi} \right]. \quad (\text{S158})$$

In general, it is not easy to derive an analytical formula for $g(C, \mu)$. Here we focus on the special case $C = 0$, which yields

$$\begin{aligned} g^*(\mu) &= \max_{0 \leq \alpha \leq \pi/2} \left[p \cos \alpha + \frac{2(1-p)}{\pi} \sin \alpha \right] \\ &= \sqrt{p^2 + \frac{4(1-p)^2}{\pi^2}} = \sqrt{\frac{(4 + \pi^2)p^2 - 8p + 4}{\pi^2}}. \end{aligned} \quad (\text{S159})$$

The minimum of $g^*(\mu)$ is attained when $p = 4/(4 + \pi^2)$, in which case we have

$$g^*(\mu) = \frac{2}{\sqrt{4 + \pi^2}}, \quad \gamma_2^*(\mu) = \frac{1}{2} + \frac{1}{\sqrt{4 + \pi^2}}. \quad (\text{S160})$$

This protocol is referred to as the equator+Z protocol. In addition, by virtue of Theorem 2 we can deduce that

$$\hat{\gamma}_2(C, \mu) = \frac{1+C}{2} + \frac{1-C}{\sqrt{4 + \pi^2}}. \quad (\text{S161})$$

The above discussion yields the following proposition.

Proposition 6. *Suppose μ is supported on the equator of the Bloch sphere together with the north and south poles. Then*

$$g^*(\mu) \geq \frac{2}{\sqrt{4 + \pi^2}}, \quad \gamma_2^*(\mu) \geq \frac{1}{2} + \frac{1}{\sqrt{4 + \pi^2}}, \quad (\text{S162})$$

$$\hat{\gamma}_2(C, \mu) \geq \frac{1+C}{2} + \frac{1-C}{\sqrt{4 + \pi^2}}. \quad (\text{S163})$$

All inequalities are saturated for the equator+Z protocol.

By contrast, the protocol corresponding to $p = 1/3$ is referred to as the equator+Z_{II}-protocol. This protocol is interesting because it is balanced and is optimal in the limit $C \rightarrow 1$ if we only consider pure states. However, it is not optimal when $C = 0$, in which case we have

$$g^*(\mu) = \frac{\sqrt{16 + \pi^2}}{3\pi}, \quad \gamma_2^*(\mu) = \frac{1}{2} + \frac{\sqrt{16 + \pi^2}}{6\pi}. \quad (\text{S164})$$

This example shows that the optimal equator+Z protocol depends on C , and no choice of p is optimal for all values of C . Compared with $\hat{\gamma}_2(C, \mu)$, the behavior of $\gamma_2(C, \mu)$ is more complicated, and it may be difficult to compare the performances of different verification protocols based on $\gamma_2(C, \mu)$. Nevertheless, the choices $p = 4/(4 + \pi^2)$ and $p = 1/3$ are both nearly optimal for all values of C .

Polygon+Z protocols

The polygon+Z protocol is constructed by replacing the uniform distribution on the equator in the equator+Z protocol with the uniform distribution on the vertices of a regular polygon. Let p be the total probability assigned to the north and south poles and let M be the number of vertices of the polygon. Then $g(C, \mu)$ is determined by the three parameters C, M, p ; therefore, it is more informative to write $g(C, \{M, p\})$ and $g^*(\{M, p\})$ in place of $g(C, \mu)$ and $g^*(\mu)$, respectively. The following proposition determines the value of $g^*(\{M, p\})$.

Proposition 7. *Suppose $0 \leq p \leq 1$ and $M \geq 3$ is an integer. Then*

$$g^*(\{M, p\}) = \begin{cases} \sqrt{p^2 + \frac{4(1-p)^2}{M^2 \sin^2(\frac{\pi}{M})}} & M \text{ even,} \\ \sqrt{p^2 + \frac{(1-p)^2}{M^2 \sin^2(\frac{\pi}{2M})}} & M \text{ odd.} \end{cases} \quad (\text{S165})$$

In the special case $p = 0$, the Polygon+Z protocol reduces to the Polygon protocol, and Proposition 7 reduces to Proposition 5 as expected.

Proof. By virtue of Eq. (S103) we can deduce the following result,

$$\begin{aligned} g^*(\{M, p\}) &= \max_{\mathbf{v}} \left(p |\hat{\mathbf{z}} \cdot \mathbf{v}| + \frac{1-p}{M} \sum_{j=1}^M |\mathbf{r}_j \cdot \mathbf{v}| \right) \\ &= \max_{0 \leq \alpha \leq \frac{\pi}{2}} \left[p \cos \alpha + \frac{1-p}{M} (\sin \alpha) \max_{\mathbf{u}} \sum_{j=1}^M |\mathbf{r}_j \cdot \mathbf{u}| \right], \end{aligned} \quad (\text{S166})$$

where the maximization in the brackets in the second line is taken over all unit vectors in the xy -plane, and the result is tied to the counterpart for the polygon protocol. Therefore,

$$\begin{aligned} g^*(\{M, p\}) &= \max_{0 \leq \alpha \leq \pi/2} [p \cos \alpha + (1-p)g^*(M) \sin \alpha] \\ &= \sqrt{p^2 + (1-p)^2 g^*(M)^2}, \end{aligned} \quad (\text{S167})$$

where $g^*(M)$ is presented in Eq. (S149). By inserting the explicit expression for $g^*(M)$, we can derive Eq. (S165) immediately, which completes the proof of Proposition 7. \square

To determine the optimal Polygon+Z protocol and the corresponding probability p_{opt} of performing Z measurement in the case $C = 0$, we need to minimize $g^*(\{M, p\})$ over p . Simple calculation based on Proposition 7 shows that

$$\begin{aligned} \min_p g^*(\{M, p\}) &= g^*(\{M, p_{\text{opt}}\}) \\ &= \begin{cases} [1 + \frac{1}{4} M^2 \sin^2(\frac{\pi}{M})]^{-1/2} & M \text{ even,} \\ [1 + M^2 \sin^2(\frac{\pi}{2M})]^{-1/2} & M \text{ odd,} \end{cases} \end{aligned} \quad (\text{S168})$$

where

$$p_{\text{opt}} := \begin{cases} [1 + \frac{1}{4} M^2 \sin^2(\frac{\pi}{M})]^{-1} & M \text{ even,} \\ [1 + M^2 \sin^2(\frac{\pi}{2M})]^{-1} & M \text{ odd,} \end{cases} \quad (\text{S169})$$

is the desired optimal probability.

In conjunction with Theorem 1 in the main text, we can now determine the optimal threshold in the guessing probability, with the result

$$\gamma_2^*(\{M, p_{\text{opt}}\}) = \begin{cases} \frac{1}{2} + [4 + M^2 \sin^2(\frac{\pi}{M})]^{-1/2} & M \text{ even,} \\ \frac{1}{2} + [4 + 4M^2 \sin^2(\frac{\pi}{2M})]^{-1/2} & M \text{ odd.} \end{cases} \quad (\text{S170})$$

By virtue of Theorem 2 we can further deduce that

$$\hat{\gamma}_2(C, \{M, p_{\text{opt}}\}) = \begin{cases} \frac{1+C}{2} + (1-C) [4 + M^2 \sin^2(\frac{\pi}{M})]^{-1/2} & M \text{ even,} \\ \frac{1+C}{2} + (1-C) [4 + 4M^2 \sin^2(\frac{\pi}{2M})]^{-1/2} & M \text{ odd.} \end{cases} \quad (\text{S171})$$

In the limit $M \rightarrow \infty$, the polygon+Z protocol approaches the equator+Z protocol; accordingly, the above results converge to the counterparts of the equator+Z protocol. For example,

$$\lim_{M \rightarrow \infty} g^*(\{M, p\}) = \sqrt{p^2 + \frac{4(1-p)^2}{\pi^2}}, \quad \lim_{M \rightarrow \infty} p_{\text{opt}} = \frac{4}{4 + \pi^2}, \quad \lim_{M \rightarrow \infty} g^*(\{M, p_{\text{opt}}\}) = \frac{2}{\sqrt{4 + \pi^2}}, \quad (\text{S172})$$

$$\lim_{M \rightarrow \infty} \gamma_2^*(\{M, p_{\text{opt}}\}) = \frac{1}{2} + \frac{1}{\sqrt{4 + \pi^2}}, \quad \lim_{M \rightarrow \infty} \hat{\gamma}_2(C, \{M, p_{\text{opt}}\}) = \frac{1+C}{2} + \frac{1-C}{\sqrt{4 + \pi^2}}. \quad (\text{S173})$$

All these limits coincide with the corresponding results for the equator+Z protocol presented in Eqs. (S159)-(S161) as expected.

Tetrahedron, cube, and octahedron protocols

In this and the following subsections we consider verification protocols based on platonic solids. A platonic solid with M vertices can be specified by a set $\{\mathbf{r}_j\}_{j=1}^M$ of M unit vectors that correspond to the vertices. Here we assume that all measurements associated with these unit vectors are chosen with the same probability of $1/M$, which is the optimal choice according to Lemma S12. Note that the octahedron protocol is equivalent to the XYZ protocol. In addition, the cube protocol is equivalent to the tetrahedron protocol, so it suffices to consider the tetrahedron protocol here.

For the tetrahedron protocol, the verification matrix reads $\Xi(\mu) = \mathbb{I}/3$, and the bound in Lemma S2 is saturated if \mathbf{v} passes through the middle point of an edge. Therefore, we have

$$g(C, \mu) = \sqrt{\frac{1+2C^2}{3}}, \quad \gamma_2(C, \mu) = \frac{1}{2} + \frac{1}{2}\sqrt{\frac{1+2C^2}{3}}, \quad (\text{S174})$$

which are identical to the results on the XYZ protocol. On the other hand, there are only six intelligent directions instead of eight, assuming $0 \leq C < 1$. When $C = 0$, the above equation reduces to

$$g^*(\mu) = \frac{1}{\sqrt{3}}, \quad \gamma_2^*(\mu) = \frac{1}{2} + \frac{1}{2\sqrt{3}}. \quad (\text{S175})$$

By virtue of Theorem 2 we can further deduce that

$$\hat{\gamma}_2(C, \mu) = \frac{1}{6}[3 + \sqrt{3} + (3 - \sqrt{3})C]. \quad (\text{S176})$$

Here it is worth pointing out that $\gamma_2^*(\mu)$ is larger than the counterpart of the optimal polygon(3)+ Z protocol (cf. Table I). So the tetrahedron protocol is not the optimal four-setting protocol. In general, the verification protocol based on a platonic solid is not necessarily optimal among protocols with the same number of measurement settings.

Icosahedron and dodecahedron protocols

Here we consider verification protocols based on the two remaining platonic solids, namely, icosahedron and dodecahedron. Both platonic solids are center symmetric, so $g^*(\mu)$ can be determined by virtue of Lemma S13.

To be concrete, the 12 vertices of the icosahedron are chosen to be

$$\frac{(0, \pm 1, \pm \tau)^T}{\sqrt{1 + \tau^2}}, \quad \frac{(\pm \tau, 0, \pm 1)^T}{\sqrt{1 + \tau^2}}, \quad \frac{(\pm 1, \pm \tau, 0)^T}{\sqrt{1 + \tau^2}}, \quad (\text{S177})$$

where $\tau = (1 + \sqrt{5})/2$ is the golden ratio. According to Lemma S13, to derive $g^*(\mu)$, it suffices to compare $|\boldsymbol{\eta}(S)|$ [cf. Eq. (S106)] for all subsets S that contain six vertices

on the same side of a plane passing through the origin. Note that an optimal set S contains one and only one vertex in each pair of antipodal vertices. For any plane passing through the origin, there exists at least one face of the icosahedron on each side of the plane. Therefore, we can choose three vertices on the same face as fixed elements of S and then choose one vertex from each of the remaining three pairs of antipodal vertices. There are $2^3 = 8$ different choices, but only three equivalent classes under orthogonal transformations. Moreover, in one of the classes, the vertices in each set are not on the same side of a plane passing through the origin. Therefore, it suffices to compute $|\boldsymbol{\eta}(S)|$ for the remaining two cases:

1. S contains six vertices, one of which is adjacent to the other five. In this case we have

$$|\boldsymbol{\eta}(S)| = 2\sqrt{\frac{2\tau^2 + 2\tau + 1}{\tau^2 + 1}} = 1 + \sqrt{5} \approx 3.236. \quad (\text{S178})$$

2. The six vertices contained in S are on one face (labeled by A) of the icosahedron and the three faces adjacent to A . In this case we have

$$|\boldsymbol{\eta}(S)| = 2\sqrt{\frac{(\tau + 1)^2 + 1}{\tau^2 + 1}} \approx 2.947. \quad (\text{S179})$$

By comparison, $|\boldsymbol{\eta}(S)|$ attains the maximum in the first case, so we have

$$g^*(\mu) = \frac{2}{12} \max_S |\boldsymbol{\eta}(S)| = \frac{1 + \sqrt{5}}{6} \approx 0.539 \quad (\text{S180})$$

by Eq. (S110). Accordingly, a unit vector is an intelligent direction at $C = 0$ iff it corresponds to one of the 12 vertices of the icosahedron.

As immediate corollaries of Eq. (S180), we can derive

$$\gamma_2^*(\mu) = \frac{7 + \sqrt{5}}{12} \approx 0.770, \quad (\text{S181})$$

$$\hat{\gamma}_2(C, \mu) = \frac{1}{12}[7 + \sqrt{5} + (5 - \sqrt{5})C]. \quad (\text{S182})$$

Incidentally, these results are very close to the counterparts of the equator+ Z_{II} -protocol.

For the icosahedron protocol, numerical calculation indicates that each intelligent direction at $C = 0$ is still an intelligent direction for $C > 0$. In other words, Eq. (6) in the main text is maximized when \mathbf{v} corresponds to one vertex of the icosahedron. This observation leads to the following conjecture.

Conjecture 2. *The icosahedron protocol μ satisfies the following equations,*

$$g(C, \mu) = \frac{1 + \sqrt{5(1 + 4C^2)}}{6}, \quad (\text{S183})$$

$$\gamma_2(C, \mu) = \frac{7 + \sqrt{5(1 + 4C^2)}}{12}. \quad (\text{S184})$$

When $0 \leq C < 1$, any intelligent direction corresponds to a vertex of the icosahedron, and vice versa.

Next, we consider the dodecahedron protocol. To be concrete, the 10 pairs of antipodal vertices of the dodecahedron are chosen to be

$$\begin{aligned} \frac{1}{\sqrt{3}}(0, \pm\tau, \pm\frac{1}{\tau})^T, \quad \frac{1}{\sqrt{3}}(\pm\frac{1}{\tau}, 0, \pm\tau)^T, \\ \frac{1}{\sqrt{3}}(\pm\tau, \pm\frac{1}{\tau}, 0)^T, \quad \frac{1}{\sqrt{3}}(\pm 1, \pm 1, \pm 1)^T. \end{aligned} \quad (\text{S185})$$

Thanks to Lemma S13 again, to derive $g^*(\mu)$ for this protocol, it suffices to compare $|\boldsymbol{\eta}(S)|$ for all subsets S that contain 10 vertices located on the same side of a plane passing through the origin. In addition, any optimal set S contains one and only one vertex in each of the 10 pairs of antipodal vertices. Note that for any plane that passes through the origin, there is at least one face of the dodecahedron on each side of the plane. Therefore, we can choose five vertices on the same face as fixed elements of S , and then choose one vertex from each of the remaining five pairs. There are $2^5 = 32$ different choices, but only seven equivalent classes. Moreover, in four of the seven classes, the vertices in each set are not on the same side of a plane passing through the origin. So it suffices to compare $|\boldsymbol{\eta}(S)|$ for the remaining three classes:

1. The 10 vertices contained in S are on three faces of the dodecahedron which are mutually adjacent. In this case we have

$$|\boldsymbol{\eta}(S)| = 2\sqrt{\frac{(\tau+2+1/\tau)^2 + \tau^2}{3}} = 3 + \sqrt{5} \approx 5.236. \quad (\text{S186})$$

2. S contains 10 vertices, five of which are on one face (labeled by A) of the dodecahedron, and each of the other five vertices is adjacent to a vertex of A . In this case we have

$$|\boldsymbol{\eta}(S)| = 2\sqrt{\frac{(\tau+1/\tau)^2 + (\tau+2)^2}{3}} \approx 4.911. \quad (\text{S187})$$

2. S contains 10 vertices. Five of them are on one face (labeled by A) of the dodecahedron; four of them are adjacent to four vertices of A , respectively. The last element of S is the antipodal point of a vertex that is adjacent to A . In this case we have

$$|\boldsymbol{\eta}(S)| = 2\sqrt{\frac{(\tau+2)^2 + 2\tau^2}{3}} \approx 4.943. \quad (\text{S188})$$

By comparison, $|\boldsymbol{\eta}(S)|$ attains the maximum in the first case, so we have

$$g^*(\mu) = \frac{2}{20} \max_S |\boldsymbol{\eta}(S)| = \frac{3 + \sqrt{5}}{10} \approx 0.524 \quad (\text{S189})$$

by Eq. (S110). Accordingly, a unit vector is an intelligent direction at $C = 0$ iff it corresponds to one of the 20 vertices of the dodecahedron.

As immediate corollaries of Eq. (S189), we can deduce

$$\gamma_2^*(\mu) = \frac{13 + \sqrt{5}}{20} \approx 0.762, \quad (\text{S190})$$

$$\hat{\gamma}_2(C, \mu) = \frac{1}{20} [13 + \sqrt{5} + (7 - \sqrt{5})C]. \quad (\text{S191})$$

Numerical calculation indicates that each intelligent direction at $C = 0$ is still an intelligent direction for $C > 0$. In other words, Eq. (6) in the main text is maximized when \mathbf{v} corresponds to one vertex of the dodecahedron. This observation leads to the following conjecture in analogy to Conjecture 2.

Conjecture 3. *The dodecahedron protocol μ satisfies the following equations,*

$$g(C, \mu) = \frac{1 + \sqrt{5 + 4C^2} + 2\sqrt{1 + 8C^2}}{10}, \quad (\text{S192})$$

$$\gamma_2(C, \mu) = \frac{11 + \sqrt{5 + 4C^2} + 2\sqrt{1 + 8C^2}}{20}. \quad (\text{S193})$$

When $0 \leq C < 1$, any intelligent direction corresponds to a vertex of the dodecahedron, and vice versa.

SUPPLEMENTARY NOTE 10: VERIFICATION OF GHZ STATES

According to the main text, each verification protocol of the Bell state is determined by a probability distribution on the Bloch sphere, which specifies the probability of performing each projective measurement. In addition, each projective measurement is specified by a unit vector on the Bloch sphere. To verify the n -qubit GHZ state

$$|G^n\rangle = \frac{1}{\sqrt{2}}(|0\rangle^{\otimes n} + |1\rangle^{\otimes n}), \quad n \geq 3, \quad (\text{S194})$$

we can simulate projective tests for the Bell state by local projective measurements on individual qubits. However, not all projective tests for the Bell state can be simulated in this way. To clarify this limitation, we need to introduce an additional concept.

Compatible measurements

Local projective measurements on the n qubits of the GHZ state $|G^n\rangle$ can be specified by a set of n unit vectors $\{\mathbf{r}_1, \mathbf{r}_2, \dots, \mathbf{r}_n\}$, where \mathbf{r}_j determines the local projective measurement on qubit j . The set $\{\mathbf{r}_1, \mathbf{r}_2, \dots, \mathbf{r}_n\}$ and the corresponding measurements are *compatible* if each qubit j has only two possible reduced states conditioned on the outcomes of all projective measurements on the other qubits when the target GHZ state is prepared; in addition, the two possible reduced states happen to be the eigenstates of $\mathbf{r}_j \cdot \boldsymbol{\sigma}$, that is, $(\mathbb{1} \pm \mathbf{r}_j \cdot \boldsymbol{\sigma})/2$. Here the compatibility requirement guarantees that the two reduced

states of qubit j can be distinguished with certainty by performing the projective measurement associated with the Bloch vector \mathbf{r}_j . In addition, given the measurement outcomes of other qubits, measurement of the remaining qubit will yield one outcome with certainty, which corresponds to passing the test. In this way, the local projective measurements specified by the set $\{\mathbf{r}_1, \mathbf{r}_2, \dots, \mathbf{r}_n\}$ can be used to construct a nontrivial test for the GHZ state $|G^n\rangle$ in which no projective measurement on any qubit is redundant.

Conversely, if the set $\{\mathbf{r}_1, \mathbf{r}_2, \dots, \mathbf{r}_n\}$ is not compatible, then the measurement outcome of some party is unpredictable even if the measurement outcomes of all other parties are known. Consequently, any outcome reported by this party would pass the test, and such a test is not useful in the presence of dishonest parties. To construct tests for verifying the GHZ state, therefore, we can focus on compatible measurements, whose properties are clarified in the following lemma.

Lemma S14. *The set $\{\mathbf{r}_1, \mathbf{r}_2, \dots, \mathbf{r}_n\}$ of local projective measurements is compatible iff either one of the following two conditions holds:*

1. $\mathbf{r}_j = (0, 0, \pm 1)^T$ for each j .
2. $\mathbf{r}_j = (\cos \phi_j, \sin \phi_j, 0)^T$ with $\sum_j \phi_j = 0 \pmod{\pi}$.

Here the condition $\sum_j \phi_j = 0 \pmod{\pi}$ means $\sum_j \phi_j$ is an integer multiple of π . Note that $-\mathbf{r}_j$ and \mathbf{r}_j correspond to the same projective measurement, except for the labeling of the two outcomes. By replacing some \mathbf{r}_j with $-\mathbf{r}_j$ if necessary, the two conditions in Lemma S14 can be simplified as

1. $\mathbf{r}_j = (0, 0, 1)^T$ for each j .
2. $\mathbf{r}_j = (\cos \phi_j, \sin \phi_j, 0)^T$ with $\sum_j \phi_j = 0 \pmod{2\pi}$.

The two types of compatible measurements determined in Lemma S14 can be used to construct two types of tests for verifying the GHZ state.

Proof of Lemma S14. If either one of the two conditions in Lemma S14 holds, then it is easy to verify that the set $\{\mathbf{r}_1, \mathbf{r}_2, \dots, \mathbf{r}_n\}$ of local projective measurements is compatible.

Conversely, suppose the set $\{\mathbf{r}_1, \mathbf{r}_2, \dots, \mathbf{r}_n\}$ is compatible. If each Bloch vector \mathbf{r}_j lies on the equator and thus has the form $(\cos \phi_j, \sin \phi_j, 0)^T$ for some azimuthal angle ϕ_j , then the two eigenstates of the operator $\mathbf{r}_j \cdot \boldsymbol{\sigma}$ read $(|0\rangle \pm e^{i\phi_j}|1\rangle)/\sqrt{2}$. After the projective measurements of all parties except for party k , the two possible reduced states of party k read

$$\frac{1}{\sqrt{2}}(|0\rangle \pm e^{i\phi_k - i\varphi}|1\rangle), \quad \varphi = \sum_{j=1}^n \phi_j. \quad (\text{S195})$$

Note that the two states are the eigenstates of $\mathbf{r}_k \cdot \boldsymbol{\sigma}$ iff $\varphi = 0 \pmod{\pi}$. So condition 2 in Lemma S14 holds.

Next, suppose at least one \mathbf{r}_j , say \mathbf{r}_1 , does not lie on the equator. Then $\mathbf{r}_1 = (\sin \theta \cos \phi, \sin \theta \sin \phi, \cos \theta)^T$ with $0 \leq \theta \leq \pi$, $0 \leq \phi < 2\pi$, and $\theta \neq \pi/2$. The two eigenstates of the operator $\mathbf{r}_1 \cdot \boldsymbol{\sigma}$ have the form

$$|\psi_+\rangle = \cos \frac{\theta}{2}|0\rangle + \sin \frac{\theta}{2}e^{i\phi}|1\rangle, \quad (\text{S196})$$

$$|\psi_-\rangle = -\sin \frac{\theta}{2}|0\rangle + \cos \frac{\theta}{2}e^{i\phi}|1\rangle. \quad (\text{S197})$$

After the projective measurement on the first qubit, the two possible reduced states of the remaining $n-1$ qubits are given by

$$|\Psi_+\rangle = \cos \frac{\theta}{2}|0\rangle^{\otimes(n-1)} + \sin \frac{\theta}{2}e^{-i\phi}|1\rangle^{\otimes(n-1)}, \quad (\text{S198})$$

$$|\Psi_-\rangle = -\sin \frac{\theta}{2}|0\rangle^{\otimes(n-1)} + \cos \frac{\theta}{2}e^{-i\phi}|1\rangle^{\otimes(n-1)}. \quad (\text{S199})$$

The reduced state of $|\Psi_+\rangle$ for each qubit $j = 2, 3, \dots, n$ reads

$$\rho_+ = \cos^2 \frac{\theta}{2}|0\rangle\langle 0| + \sin^2 \frac{\theta}{2}|1\rangle\langle 1|. \quad (\text{S200})$$

By contrast, the reduced state of $|\Psi_-\rangle$ for each qubit $j = 2, 3, \dots, n$ reads

$$\rho_- = \sin^2 \frac{\theta}{2}|0\rangle\langle 0| + \cos^2 \frac{\theta}{2}|1\rangle\langle 1|. \quad (\text{S201})$$

By assumption ρ_+ is a convex combination of the two eigenstates of $\mathbf{r}_j \cdot \boldsymbol{\sigma}$ for each $j = 2, 3, \dots, n$, and so is ρ_- . It follows that $\mathbf{r}_j = (0, 0, \pm 1)^T$ for $j = 2, 3, \dots, n$. Accordingly, the two possible reduced states of qubit 1 conditioned on the measurement outcomes of the other $n-1$ qubits are $|0\rangle\langle 0|$ and $|1\rangle\langle 1|$, which implies that $\mathbf{r}_1 = (0, 0, \pm 1)^T$. Therefore, all \mathbf{r}_j are parallel to the unit vector $(0, 0, 1)^T$, and condition 1 in Lemma S14 holds. This observation completes the proof of Lemma S14. \square

Tests and protocols for verifying GHZ states

Recall that \mathcal{H} is the set of honest parties, and $V_{\mathcal{H}}$ is the two-dimensional subspace spanned by $|0\rangle_{\mathcal{H}}$ and $|1\rangle_{\mathcal{H}}$, where

$$|0\rangle_{\mathcal{H}} = \bigotimes_{j \in \mathcal{H}} |0\rangle_j, \quad |1\rangle_{\mathcal{H}} = \bigotimes_{j \in \mathcal{H}} |1\rangle_j. \quad (\text{S202})$$

Let $P_{\mathcal{H}}$ be the projector onto $V_{\mathcal{H}}$ and let $\mathbb{I}_{\mathcal{H}}$ be the identity operator on the Hilbert space associated with \mathcal{H} . To simplify the terminology, all parties other than the honest parties will be referred to as the adversary. Without loss of generality, we can assume that the actual state ρ to be verified is prepared by the adversary. Let $\rho_{\mathcal{H}} := \text{tr}_{\mathcal{D}}(\rho)$ be the reduced state of ρ for the honest parties.

The two types of compatible measurements determined in Lemma S14 can be used to construct two types of

tests for verifying the GHZ state. In the first type, all parties perform Z measurements, and the test is passed if they obtain the same outcome. In the perspective of the honest parties, including the verifier, these measurements realize the three-outcome projective measurement

$$\{|0\rangle_{\mathcal{H}}\langle 0|, |1\rangle_{\mathcal{H}}\langle 1|, \mathbb{I}_{\mathcal{H}} - P_{\mathcal{H}}\}. \quad (\text{S203})$$

The state ρ prepared by the adversary is rejected immediately if the third outcome occurs. To maximize the guessing probability, it is advantageous for the adversary to prepare the state ρ such that $\rho_{\mathcal{H}}$ is supported in $V_{\mathcal{H}}$. Then the verifier effectively realizes the Z measurement on $V_{\mathcal{H}}$.

In the second type of tests, party j performs the $X(\phi_j)$ measurement with $\sum_j \phi_j = 0 \pmod{2\pi}$, where

$$X(\phi_j) := \begin{pmatrix} 0 & e^{-i\phi_j} \\ e^{i\phi_j} & 0 \end{pmatrix} \quad (\text{S204})$$

corresponds to the Bloch vector $(\cos \phi_j, \sin \phi_j, 0)^T$. The test is passed if the number of outcome -1 is even. In the perspective of the honest parties, these measurements realize the projective measurement with two outcomes

$$P_{\pm}(\{\phi_j\}_j) = \frac{\mathbb{I}_{\mathcal{H}} \pm \bigotimes_{j \in \mathcal{H}} X(\phi_j)}{2}. \quad (\text{S205})$$

Let $\phi_{\mathcal{H}} = \sum_{j \in \mathcal{H}} \phi_j \pmod{2\pi}$. In the subspace $V_{\mathcal{H}}$, this measurement reduces to a projective measurement with two outcomes

$$P_{\pm}^{\mathcal{H}} = \frac{P_{\mathcal{H}} \pm X_{\mathcal{H}}(\phi_{\mathcal{H}})}{2}, \quad (\text{S206})$$

where

$$X_{\mathcal{H}}(\phi_{\mathcal{H}}) = e^{-i\phi_{\mathcal{H}}} |0\rangle_{\mathcal{H}}\langle 1| + e^{i\phi_{\mathcal{H}}} |1\rangle_{\mathcal{H}}\langle 0|. \quad (\text{S207})$$

So the verifier can effectively realize the $X(\phi_{\mathcal{H}})$ measurement on $V_{\mathcal{H}}$. If $\rho_{\mathcal{H}}$ is supported in $V_{\mathcal{H}}$, then the guessing probability is the same as in the verification of the Bell state. However, it is not clear whether the adversary can increase the guessing probability if $\rho_{\mathcal{H}}$ is not supported in $V_{\mathcal{H}}$. To eliminate this problem, we can introduce some randomness in each ϕ_j .

Suppose $\phi_1, \phi_2, \dots, \phi_n$ are chosen independently and uniformly at random from the interval $[0, 2\pi)$; then $\phi_{\mathcal{H}}$ is uniformly distributed in $[0, 2\pi)$. Given $\phi \in [0, 2\pi)$, the average of $\bigotimes_{j \in \mathcal{H}} X(\phi_j)$ under the condition $\phi_{\mathcal{H}} = \phi$

reads

$$\left\langle \bigotimes_{j \in \mathcal{H}} X(\phi_j) \right\rangle_{\phi} = X_{\mathcal{H}}(\phi), \quad (\text{S208})$$

which implies that

$$\begin{aligned} Q_{\pm} &:= \langle P_{\pm}(\{\phi_j\}_j) \rangle_{\phi} = \frac{\mathbb{I}_{\mathcal{H}} \pm X_{\mathcal{H}}(\phi_{\mathcal{H}})}{2} \\ &= \frac{P_{\mathcal{H}} \pm X_{\mathcal{H}}(\phi_{\mathcal{H}})}{2} + \frac{\mathbb{I}_{\mathcal{H}} - P_{\mathcal{H}}}{2}. \end{aligned} \quad (\text{S209})$$

In this way the verifier can effectively realize the $X(\phi)$ measurement on $V_{\mathcal{H}}$, where ϕ is completely random. The resulting verification protocol corresponds to the equator protocol in the verification of the Bell state. Thanks to the following equality

$$(\mathbb{I} - P_{\mathcal{H}})Q_{+}(\mathbb{I} - P_{\mathcal{H}}) = (\mathbb{I} - P_{\mathcal{H}})Q_{-}(\mathbb{I} - P_{\mathcal{H}}), \quad (\text{S210})$$

the adversary cannot gain any advantage if $\rho_{\mathcal{H}}$ is not supported in $V_{\mathcal{H}}$, and the maximum guessing probability is the same as in the verification of the Bell state. Equator+ Z protocol can be constructed by adding the Z measurement.

Let $M \geq 3$ be an integer. If $\phi_1, \phi_2, \dots, \phi_n$ are chosen independently and uniformly at random from the discrete set $\{2k\pi/M\}_{k=0}^{M-1}$; then $\phi_{\mathcal{H}}$ is uniformly distributed in the same set. In addition, Eqs. (S208) and (S209) still hold for any $\phi \in \{2k\pi/M\}_{k=0}^{M-1}$. In this way the verifier can effectively realize the polygon protocol for verifying the GHZ state. Again the adversary cannot gain any advantage if $\rho_{\mathcal{H}}$ is not supported in $V_{\mathcal{H}}$, and the maximum guessing probability is the same as in the verification of the Bell state. Polygon+ Z protocol can be constructed by adding the Z measurement.

In summary, each verification protocol of the n -qubit GHZ state corresponds to a probability distribution on the Bloch sphere which is supported on the equator together with the north and south poles. Moreover, the equator protocol, equator+ Z protocol, polygon protocols, and polygon+ Z protocols (including the XYZ protocol) can be generalized to GHZ states such that the guessing probabilities and sample efficiencies are identical to the counterparts for the verification of the Bell state. Notably, GHZ states can be verified almost as efficiently as Bell states. The simplest verification protocol is the XY protocol, which is equivalent to the polygon protocol with four vertices. The optimal protocol is an equator+ Z protocol, in which the optimal probability p_Z for performing the Z measurement depends on the target fidelity F as in the verification of the Bell state.

SUPPLEMENTARY REFERENCES

- [1] Šupić, I. & Hoban, M. J. Self-testing through EPR-steering. *New J. Phys.* **18**, 075006 (2016).
- [2] Gheorghiu, A., Wallden, P. & Kashefi, E. Rigidity of quantum steering and one-sided device-independent verifiable quantum computation. *New J. Phys.* **19**, 023043 (2017).
- [3] Pappa, A., Chailloux, A., Wehner, S., Diamanti, E. & Kerenidis, I. Multipartite Entanglement Verification Resistant against Dishonest Parties. *Phys. Rev. Lett.* **108**, 260502 (2012).
- [4] McCutcheon, W. et al. Experimental verification of multipartite entanglement in quantum networks. *Nat. Commun.* **7**, 13251 (2016).
- [5] Pallister, S., Linden, N. & Montanaro, A. Optimal Verification of Entangled States with Local Measurements. *Phys. Rev. Lett.* **120**, 170502 (2018).
- [6] Zhu, H. & Hayashi, M. Efficient Verification of Pure Quantum States in the Adversarial Scenario. *Phys. Rev. Lett.* **123**, 260504 (2019).
- [7] Zhu, H. & Hayashi, M. General framework for verifying pure quantum states in the adversarial scenario. *Phys. Rev. A* **100**, 062335 (2019).
- [8] Dimić, A., Šupić, I. & Dakić, B. Sample-efficient device-independent quantum state verification and certification. Preprint at <http://arxiv.org/abs/2105.05832> (2021).
- [9] Mayers, D. & Yao, A. Self Testing Quantum Apparatus, *Quantum Inf. Comput.* **4**, 273 (2004).
- [10] Šupić, I. & Bowles, J. Self-testing of quantum systems: a review. *Quantum* **4**, 337 (2020).
- [11] Hayashi, M., Matsumoto, K. & Tsuda, Y. A study of LOCC-detection of a maximally entangled state using hypothesis testing. *J. Phys. A: Math. Gen.* **39**, 14427–14446 (2006).
- [12] Zhu, H. & Hayashi, M. Optimal verification and fidelity estimation of maximally entangled states. *Phys. Rev. A* **99**, 052346 (2019).
- [13] Li, Z., Han, Y.-G. & Zhu, H. Optimal Verification of Greenberger-Horne-Zeilinger States. *Phys. Rev. Appl.* **13**, 054002 (2020).
- [14] Clauser, J. F., Horne, M. A., Shimony, A. & Holt, R. A. Proposed Experiment to Test Local Hidden-Variable Theories. *Phys. Rev. Lett.* **23**, 880–884 (1969).
- [15] McKague, M., Yang, T. H. & Scarani, V. Robust self-testing of the singlet. *J. Phys. A: Math. Theor.* **45**, 455304 (2012).
- [16] Mermin, N. D. Extreme Quantum Entanglement in a Superposition of Macroscopically Distinct State. *Phys. Rev. Lett.* **65**, 1838 (1990).
- [17] Kaniewski, J. Analytic and Nearly Optimal Self-Testing Bounds for the Clauser-Horne-Shimony-Holt and Mermin Inequalities. *Phys. Rev. Lett.* **117**, 070402 (2016).